



Published in final edited form as:

*Prog Retin Eye Res.* 2018 January ; 62: 58–76. doi:10.1016/j.preteyeres.2017.10.001.

## Development of the hyaloid, choroidal and retinal vasculatures in the fetal human eye

Gerard A. Luttý\*,<sup>1</sup> and D. Scott McLeod<sup>1</sup>

Wilmer Ophthalmological Institute, Baltimore, MD 21287, United States

### Abstract

The development of the ocular vasculatures is perfectly synchronized to provide the nutritional and oxygen requirements of the forming human eye. The fetal vasculature of vitreous, which includes the hyaloid vasculature, vasa hyaloidea propria, and tunica vasculosa lentis, initially develops around 4–6 weeks gestation (WG) by hemo-vasculogenesis (development of blood and blood vessels from a common progenitor, the hemangioblast). This transient fetal vasculature expands around 12 WG by angiogenesis (budding from primordial vessels) and remains until a retinal vasculature begins to form. The fetal vasculature then regresses by apoptosis with the assistance of macrophages/hyalocytes. The human choroidal vasculature also forms by a similar process and will supply nutrients and oxygen to outer retina. This lobular vasculature develops in a dense collagenous tissue juxtaposed with a cell constitutively producing vascular endothelial growth factor (VEGF), the retinal pigment epithelium. This epithelial/endothelial relationship is critical in maintaining the function of this vasculature throughout life and maintaining its fenestrated state. The lobular capillary system (choriocapillaris) develops first by hemo-vasculogenesis and then the intermediate choroidal blood vessels form by angiogenesis, budding from the choriocapillaris. The human retinal vasculature is the last to develop. It develops by vasculogenesis, assembly of CXCR4<sup>+</sup>/CD39<sup>+</sup> angioblasts or vascular progenitors perhaps using Muller cell Notch1 or axonal neuropilin-1 for guidance of semaphorin 3A-expressing angioblasts. The fovea never develops a retinal vasculature, which is probably due to the foveal avascular zone area of retina expressing high levels of anti-angiogenic factors. From these studies, it is apparent that development of the mouse ocular vasculatures is not representative of the development of the human fetal, choroidal and retinal vasculatures.

### Keywords

Angioblasts; Hemangioblasts; Choriocapillaris; Endothelial cells; Hemovasculogenesis; Hyaloid vasculature; Pericytes; Retina; Vasculogenesis

### 1. Introduction

Development of the vasculatures in the embryonic and fetal human eye is an orchestrated, synchronous process that is dependent on the oxygen demand of the developing tissue. The

\*Corresponding author. M041 Smith Building, 400 North Broadway, Baltimore, MD 21287 United States. gluttý@jhmi.edu (G.A. Luttý).

<sup>1</sup>Percentage of work contributed by each author in the production of the manuscript is as follows: Luttý 50%, McLeod 50%.

elegant work of Ida Mann suggested that the choroidal vasculature develops first and then the fetal vasculature of vitreous and finally the retinal vasculature (Mann, 1928). A thorough investigation of the development of the ocular vasculatures in the human has not been done since the work of Mann. The goal of this manuscript was to review recent studies of these events, which used modern immunohistochemical, biochemical, and molecular techniques. Our approach was to examine the chronological development of the three vascular systems starting at 5 weeks gestation. The development of the vasculature in each compartment or niche is described separately due the complexity and uniqueness of the developmental events in each niche.

## **2. Fetal vasculature of vitreous: hyaloid vasculature, tunica vasculosa lentis and vasa hyaloidea propria**

### **2.1. Five and one half through six weeks gestation (WG)**

The eyecup forms and the fissure closes at 5.5 WG (Mann, 1928). Undifferentiated mesenchymal cells invade the future vitreous space through the annular opening between the optic cup and lens primordium and through the closing fissure (Balazs et al., 1980). Using Giemsa staining of glycol methacrylate sections (JB4), it was clear that some cells in the mesenchymal anlage entering through the pupillary margin were mesenchyme (blue, basophilic), while others appear to be erythroblasts, nucleated cells with acidophilic (pink) cytoplasm (Fig. 1). In serial Giemsa stained sections, these streams of cells were often composed entirely of “erythroblast” islands but, in subsequent sections, the erythroblasts were surrounded by mesenchymal cells (Fig. 2) (McLeod et al., 2012). Additional evidence for these nucleated acidophilic cells being “erythroblasts” was that some of these cells in these islands expressed epsilon hemoglobin (Hbe), embryonic globin made between 2 and 9 WGs (weeks gestation) in erythroblasts, notably in yolk sac from 2 to 6 WGs. Hbe was expressed in cells co-expressing endothelial cell markers like VEGFR2 (vascular endothelial cell receptor-2), CD31 (PECAM), and CD34 (Fig. 3). This population of cells co-expressing erythroblast and endothelial cell markers suggested that these formations were like blood islands in yolk sac (Eichmann et al., 1997). Furthermore, most of the cells in the anlage also expressed endoglin, a TGF $\beta$  receptor produced during hemangioblast specification and commitment (Fig. 4) (Perlingeiro, 2007). At 5.5 WG, serial JB4 sections demonstrated that the hyaloid artery had not entered the vitreous cavity, while islands of blood vessels were forming in vitreous, most prominently near lens capsule (Fig. 5A–B). Even at 6.5 WG, transmission electron microscopy (TEM) demonstrated that some erythroblasts were free in primordial vitreous while others were confined within islands surrounded by mesenchymal cells, suggesting assembly of blood and blood vessels components from the cells in the anlage (Fig. 6). Our observations supported the early observations of Balazs et al. that undifferentiated mesenchymal cells that invade vitreous differentiate into prevascular cells, hemangioblasts, and fibrocytes (Balazs et al., 1980). In aggregate these observations strongly suggest that the fetal vasculature of vitreous forms by hemo-vasculogenesis, development of blood vessel and all components of the blood system [hematopoietic (CD34), endothelial cells (CD31) and erythropoietic cells (Hb-*e*)] from a common precursor: the hemangioblast (Eichmann et al., 1997). Sequeira-Lopez et al. have suggested

in mouse that hemo-vasculogenesis is the mechanism for development of embryonic vasculatures in several organs (Sequeira Lopez et al., 2003).

As the tunica vasculosa lentis (TVL) of vitreous forms, so does the posterior portion, the vasa hyaloidea propria. In serial sections of a 5.5 WG whole globe, we never observed a continuous blood vessel from the closing fissure into the vitreous cavity (Fig. 5A–B). Instead we observed a fragmented hyaloid artery in the closed fissure, which agrees with Balazs' observation that the hyaloid vasculature formed in segments at 6 WG (Balazs et al., 1980). Our observation, along with Balazs', suggests organization of the mesenchymal anlage that invades through the annular opening and open fissure forms the vasa hyaloidea propria. This is in disagreement with Ida Mann's conclusion that the fetal vasculature forms by branching of the hyaloid artery (Mann, 1928). However, in Mann's elegant drawings and micrographs from Jacobiec (Jacobiec, 1982), there appears to be an anlage of mesenchyme and no formed blood vessels.

## 2.2. Seven to twelve weeks gestation

The hyaloid artery has formed by 7 WG (Fig. 5). However, there were no Ki67<sup>+</sup> cells associated with any part of the fetal vasculature, suggesting angiogenesis had not yet occurred at this stage of development (Fig. 7A–B). At this age, NG2, a pericyte marker, was observed in a few cells in blood islands. Some of these cells appeared to co-express both endothelial cell and pericyte markers (Fig. 8). Expression of NG2 increased with age and became localized exclusively to perivascular cells that appeared morphologically like mature pericytes with nuclei bulging from the outer surface of the vasculature, while the inner cells expressed only endothelial cell markers like CD31 (Fig. 8). Proliferation was observed in the vascular elements by 10 WG but it was mostly confined to perivascular cells (Fig. 7). The vasculature continued to expand and mature through 12 WG and proliferation was evident in both endothelial cells and pericytes at this stage in development (Fig. 7E & G). Capillary adventitial cells expressed NG2 (Fig. 8I–L) while the adventitial cells in the hyaloid artery and its branches expressed smooth muscle actin, an arterial marker (data not shown). In general, progenitor markers like endoglin, cKit, and CXCR4 expression declined as the vasculature matured while endothelial cell markers CD31 and vWf increased. Pericytes expressed NG2 but not smooth muscle actin (McLeod et al., 2012).

## 2.3. Regression of the fetal vasculature of vitreous

The anterior fetal vasculatures, VHP and PM, will supply oxygen and nutrients to developing lens and the VHP to inner retina until a retinal vasculature forms. Balazs et al. (1980) and Zhu and associates (Zhu et al., 1999) studied the mature fetal vasculatures of vitreous and agreed upon the cellular composition of this vasculature. Smooth muscle cells ( $\alpha$ SMA<sup>+</sup>) were not present on capillaries but were present on large blood vessels. Hyalocytes, which were major histocompatibility complex (MHC)-1 and -2 positive as well as CD45<sup>+</sup>, were closely associated with all parts of the fetal vasculature (Balazs et al., 1980; Zhu et al., 1999). The hyaloid vasculature remains intact until 13 WG. At that time, regression and apoptosis of vascular elements was apparent when TUNEL labeling was done by Zhu et al. (2000). Hyalocytes being juxtaposed with pycnotic endothelial cells suggested

that hyalocytes were involved in the regression and removal of this terminal vasculature (Zhu et al., 2000).

### 3. Choroidal vasculature

#### 3.1. Six-eleven weeks gestation: development of choriocapillaris

When the fissure closes, the retinal pigment epithelial cells have already formed a complete monolayer that has junctional complexes (Oguni et al., 1991). During this same stage of development, when mesenchyme invade the vitreous space (5–6 WG), a narrow linear arrangement of cells that expressed CD34, CD31, CD39, and VEGFR-2 was observed where the choriocapillaris will form posterior to the RPE (Fig. 9A–D). Giemsa staining of serial sections at this age, revealed similar blood island-like structures to those observed in vitreous (Hasegawa et al., 2007). As in vitreous, the islands had acidophilic nucleated erythroblasts that were within lumens or even lined lumens (Fig. 10). At the ultrastructural level, erythroblasts were free in some areas with other erythroblasts surrounded by mesenchymal precursors (Hasegawa et al., 2007). Some cells in these blood islands co-expressed Hb $\epsilon$  and endothelial cell markers like CD31 (Fig. 11). This was true in the forming CC as well as in free cells in the stroma (Fig. 11). At 6 WG, there were no Ki67<sup>+</sup> cells associated with choriocapillaris blood islands (Fig. 12A–B), suggesting that these structures formed by hemangioblast differentiation. Therefore, like the fetal vasculature of vitreous, the CC appears to form by hemo-vasculogenesis. Hb $\epsilon$  declines after 7 WG (Hasegawa et al., 2007) but, in the flat perspective, the CC appeared island-like when stained with anti-CD39 (Fig. 13A) (Hasegawa et al., 2007). Cells in the islands expressed endogenous alkaline phosphatase, which remains a characteristic of this vasculature through adult life (data not shown) (Baba et al., 2009; McLeod and Lutty, 1994). Localization of CD39 at 7 WG clearly demonstrated that the fetal human eye has a single layer of capillaries in choroid (Fig. 9E).

#### 3.2. Twelve to twenty two weeks gestation: maturation of choriocapillaris and development of the intermediate blood vessels (Sattler's layer)

By 12 WG, intermediate blood vessels begin to form and are associated with the single layer of capillaries, the choriocapillaris (Fig. 9F), and the pattern of CD39<sup>+</sup> seemed more linear (Fig. 13B). Also at 11–12 WG, there was proliferation (Ki67<sup>+</sup> cells) within the outer aspect of the immature CC and associated with the developing intermediate blood vessels that appeared to bud from the CC (Fig. 12C–D). Allende and associates also observed this proliferation on the scleral side of the choriocapillaris from 14 until 18.5 WG (Allende et al., 2006). Therefore, expansion of the choroidal vasculature into the deeper stroma appears to occur by angiogenesis, proliferation and migration of endothelial cells from existing blood vessels (Fig. 12C–D). The stages in maturation of the CC were seen with TEM in various regions of the choroid (Baba et al., 2009). In periphery, at 11 WG, there were aggregates of progenitors in which narrow slit-like lumens were present. Outer cells in the aggregate appear similar ultrastructurally to those forming lumen, suggesting the same progenitors gave rise to both endothelial cells (ECs) and pericytes (Fig. 14A). At the equator, the lumens were broader and the luminal cells made tight junctions with each other (Fig. 14B). The CC in the posterior pole were more mature with luminal cells sitting on a basement membrane

and abluminal cells having distinctly different chromatin arrangement than the luminal cells (Fig. 14C). The abluminal, pericyte-like cells even formed tongue-in-socket processes with the luminal cells, a characteristic formation of pericytes and endothelial cells (data not shown) (Baba et al., 2009).

The maturation of CC began around 12 WG when NG2 was expressed in most of the CC, although it was expressed in a few progenitors as early as 7 WG (Fig. 15). Cell type determination in the CC appeared to occur in the posterior pole first and lagged behind in periphery. It was not really until 21–22 WG that CC maturation was accomplished. At this age, there were three layers of vasculature in the submacula (Fig. 9G) and the CC pattern became more chicken-wire-like (Fig. 13C). This is not the complete adult pattern nor density of CC, so expansion of the network must occur after this age. At 22 WG there were many characteristics of adult CC. Alpha smooth muscle actin ( $\alpha$ SMA) and NG2 were expressed in arteries and veins and capillaries respectively (Fig. 15). In addition, PV-1 (a protein in the diaphragm of fenestrations) was expressed throughout the CC at this time (Fig. 16F). With TEM, continuous fenestrations were present in some areas mostly on the retinal side of CC lumens (Baba et al., 2009). Our interpretation of choroidal vascular formation is that the CC forms by hemo-vasculogenesis. As the islands of progenitors mature, progenitors will traverse between the islands eventually forming a network of capillaries without proliferation. Eventually this monolayer of capillaries will bud to form intermediate blood vessels, which we hypothesize will anastomose with larger blood vessels that are advancing from the posterior eye wall. Anastomoses of capillaries and large blood vessels to complete formation of a vascular plexus has been observed in other vasculature (Drake and Fleming, 2000). By 21–22 WG, when photoreceptors are developing inner segments and becoming metabolically active, the CC will have fenestrations and mature EC to service the developing photoreceptors (Fig. 16C, F and I).

## 4. Retinal vasculature

### 4.1. Twelve to twenty five weeks gestation

The retinal vasculature is the last of the major vascular systems in the human eye to develop. While the initial fetal vasculature of vitreous and primordial CC develop by hemo-vasculogenesis around 5–7 WG, the retina is predominantly undifferentiated. There was a broad neuroblastic layer and most inner neuroblastic layer progenitors expressed CXCR4 (Fig. 17D) (Hasegawa et al., 2008). CXCR4 is present on endothelial cells, ganglion cell precursors, hemangioblasts, and vascular progenitors (Chen et al., 2007; Kawakami et al., 2015; Wang et al., 2015). The ligand for CXCR4 is stromal derived factor-1 (SDF-1), which is hypoxia-inducible and was highly expressed in innermost retina (Fig. 17C). This suggested that there is a gradient of the chemoattractant SDF-1 from neuroblastic layer to inner retina. Although no cells in retina expressed CD31 at this time, there were progenitors in inner retina that expressed both CD39 and CXCR4 (Fig. 18). CD39 (Ectonucleoside triphosphate diphosphohydrolase-1 or NDTPase) is expressed by vascular precursors, endothelial cells, and some macrophages (Noronha-Matos et al., 2012). Because CD39 was expressed by cells in the primitive vasculatures in vitreous and choroid at this time, this suggested that individual vascular progenitors or angioblasts were present in the retina as

early as 7 WG (Fig. 18). CD39<sup>+</sup> angioblasts also co-expressed CXCR4 in the nerve fiber layer at the optic nerve (Fig. 19A–B). These cells did not express the pan leukocyte marker CD45, so they were not macrophages or microglia (data not shown) (McLeod et al., 2006). Ki67 expression was limited to the outer portion of the neuroblastic layer and not observed in inner retina (Fig. 19C–D). It was not until 12–14 WG that these angioblasts began to organize in the peripapillary region (Hasegawa et al., 2008).

The initial vasculature was simply linear columns of these CD39<sup>+</sup>/CXCR4<sup>+</sup> cells in the nerve fiber layer (Fig. 19E–F). Using NISSL staining of flat mount retinas, Chan-Ling concluded that these precursors migrated out of optic nerve and aligned on nerve fibers (Hughes et al., 2000). Ashton observed these spindle-shaped cells as well during human retinal vascular development (Ashton, 1970). Using the enzyme histochemical reaction for adenosine diphosphatase (ADPase), which is an enzyme activity now recognized as CD39, we observed angioblasts (ADPase<sup>+</sup>) in linear arrangement in the peripapillary region at 12 WG (Fig. 20). When mapped, the ADPase<sup>+</sup> cells were present in inner retina more than a mm in advance of the vascular cords that Michaelson called primordial blood vessels (Michaelson, 1948) (Fig. 20). The cells in the cords were CD34<sup>+</sup> suggesting their differentiation to EC and they were assembled in advance of GFAP<sup>+</sup>/PAX2<sup>+</sup> astrocytes (Chan-Ling et al., 2004) (Fig. 21). Chan-Ling had demonstrated previously that PAX2 was present in human retinal astrocyte precursors (Chu et al., 2001). GFAP<sup>+</sup>/PAX2<sup>+</sup> astrocytes were associated with formed CD34<sup>+</sup> blood vessels and nerve fiber bundles. Astrocyte precursors (GFAP<sup>-</sup>/PAX2<sup>+</sup>) were present at the tips of forming cords or slightly in advance (Chan-Ling et al., 2004). Eventually, the cords had lumens and it was at this point that the endothelial cells strongly expressed CD34.

At 14 WG, there was proliferation associated with the rudimentary vasculature, but all proliferating cells were PAX2<sup>+</sup> (Chan-Ling et al., 2004; McLeod et al., 2006). Sandercoe and associates observed proliferation associated with the retinal vasculature at 18 WG and the majority of the Ki67<sup>+</sup> cells were astrocytes, while the minority was in endothelial cells (CD34<sup>+</sup>) (Sandercoe et al., 1999). The superficial retinal vasculature expanded creating a butterfly-shaped pattern of CD39<sup>+</sup> blood vessels at 21 WG (Fig. 22), but the presumed macula was never vascularized in this period. Interestingly there were still solitary angioblasts in advance of blood vessels and some angioblasts were creating islands of vasculature that were not associated with the formed vasculature (Fig. 23). Hughes et al. observed that eventually the deep retinal capillary network formed by angiogenesis at 25–26 WG (Hughes et al., 2000).

#### 4.2. Maturation of the retinal vasculature

The anatomical fovea begins to form at 22 WG when there is an absence of rods in the area and the temporal arcade blood vessels advance into the presumed macula; however, foveal development will only be complete between 15 and 45 months postpartum (Hendrickson and Yuodelis, 1984). A recent OCT study concurred with this progression in macular development (Dubis et al., 2012). At 26 WG, the area is a blood vessel-free linear zone from nasal macula to ora serrata and only cones are present in the presumed fovea within this zone (Provis and Hendrickson, 2008). At 37 WG, the foveal avascular zone (FAZ) is a

complete circle. Interestingly, the FAZ decreased in size from 500  $\mu\text{m}$  at 35 WG to 150–170  $\mu\text{m}$  at 37–41 WG. Provis and Hendrickson concluded that the foveal area is never vascularized during development (Provis and Hendrickson, 2008). In monkey, they demonstrated that astrocytes also were absent in the FAZ and formed a ring encircling the FAZ during development (Provis et al., 2000). The decrease in size of the FAZ and yet the FAZ remaining avascular, they attributed to the presence in fovea of anti-angiogenic agents pigment epithelial-derived factor (PEDF) and brain natriuretic peptide precursor B (NPPB), which they found elevated in the fovea compared to other parts of the fundus (Kozulin et al., 2009b, 2010).

#### 4.3. Guidance systems for retinal vascular development (mouse versus man)

We speculate that the guidance for human vascular formation may be Muller cells and axons, not astrocytes as in mouse (Fruttiger, 2002). Even at 9 WG, the inner Muller cell processes have formed in human retina (Fig. 24A). By 12 WG Muller cells express Notch 1 (Fig. 24B–E), which has been implicated in vascular development in several organs (Roca and R.H., 2007) as well as glial differentiation (Lundkvist and Lendahl, 2001). At 17 WG, Muller cells appear to create extracellular spaces in inner retina in which the primitive blood vessels develop, very similar to our observations in forming canine retinal vasculature (Lutty and McLeod, 1987; McLeod et al., 1987; Taomoto et al., 2000) (Fig. 25). In mouse, Notch1 is expressed by monocytes that appear to provide guidance at the tips of the vasculature (Outtz et al., 2011) and in stalk endothelial cells that control formation of Jagged1<sup>+</sup> tip cells during angiogenesis (Table 1B) (Hellstrom et al., 2007).

Provis and associates demonstrated that VEGF is expressed by astrocytes in inner human retina using in situ hybridization (Provis et al., 1997). We find, using immunohistochemistry, VEGF<sub>165</sub> barely expressed at 7 WG in retina but it is more prominently expressed at 12 WG (Baba et al., 2012). At 12 WG, just as angioblast aggregation and assembly in blood vessels begins, VEGF was localized to the inner neuroblastic layer and Muller cell processes (Fig. 26). In man and mouse, the endothelial cells expressed VEGFR2, which is also expressed in human angioblasts (Chan-Ling et al., 2004). Neuropilin1 (NRP1) also binds VEGF<sub>165</sub> as well as semaphorin3A (Sema3a). In inner human retina, NRP1 was expressed by axons whereas Sema3a appeared to be expressed angioblasts and neuroblastic layer progenitors at 12 WG (Fig. 27). Larrivee et al. have highlighted the relationship between axons and vascular development that includes the presence of semaphorins (Larrivee et al., 2009). In their studies on the developing Macaque retina, Kozulin et al. suggested a role for ganglion cell layer gradients of Eph-A6 in vascular patterning (Kozulin et al., 2009a). The differences in guidance molecules between mouse and man are summarized in Table 1B.

## 5. Conclusions and future directions

The development of the three ocular vasculatures reviewed herein is perfectly synchronized to provide the nutritional and oxygen requirements of the forming human eye. The fetal vasculature of vitreous, which includes the hyaloid vasculature, vasa hyaloidea propria, and tunica vasculosa lentis, develops by hemo-vasculogenesis when the closure of the globe is nearing completion (McLeod et al., 2012). This transient fetal vasculature remains until a

retinal vasculature forms and then it regresses by apoptosis in mouse and man with the assistance of macrophages/hyalocytes (Lang et al., 1994; Lang and Bishop, 1993; Zhu et al., 2000). The human choroidal vasculature also develops by hemo-vasculogenesis and will supply nutrients and oxygen to outer retina (Table 1A). This lobular vasculature develops in a dense collagenous tissue juxtaposed with a cell constitutively making VEGF, the RPE. This will be critical in maintaining the CC and keeping it fenestrated, which has been elegantly shown in mouse (Marneros et al., 2005; Saint-Geniez et al., 2006). The retinal vasculature is the last to develop. In human it develops by vasculogenesis, assembly of CXCR4<sup>+</sup>/CD39<sup>+</sup> angioblasts or vascular progenitors perhaps using Muller cell Notch1 or axonal NRP1 for guidance of semaphorin 3A<sup>+</sup> angioblasts. The mouse retinal vasculature develops by angiogenesis using astrocytes as a template with Notch1 being in stalk endothelial cells and microglia (Table 1A). Provis has elegantly shown that fovea never has a retinal vasculature, which is probably because the FAZ area of retina has high levels of antiangiogenic factors. Therefore, mouse is desirable in studying ocular vascular development because it is genetically manipulatable. i.e. a specific gene can be knocked out or upregulated. However, the development of the mouse ocular vasculatures is not representative of the development of the human retinal and choroidal vasculatures.

Although we have presented the general progression of human ocular vascular development, many molecular details remain unknown. Although the functional details are difficult to elucidate in studies of postmortem human tissue, it is necessary to compare snapshots of gene expression seen in human tissue, as presented in this review, to that identified in mouse where functional involvement can be manipulated and proven. A wonderful example of this is the mouse studies from Jeremy Nathán's lab that demonstrate that familial exudative vitreoretinopathy in human are caused by a mutation in *frizzled4* gene (Xu et al., 2004). Understanding the triggers for regression of the fetal vasculature in vitreous could help us treat or prevent persistent fetal vasculature. It is incredibly important to understand the difference between retinal vasculogenesis versus angiogenesis in developing future therapies for retinopathy of prematurity where one needs to inhibit angiogenesis while permitting vasculogenesis (normal vascularization of the human retina) to proceed.

## Acknowledgments

The authors wish to acknowledge the dedicated and meticulous work of the following scientists in the Lutty Lab: Takayuki Baba, Imran Bhutto, Malia Edwards, Rhonda Grebe, Takuya Hasegawa, Carol Merges, Tarl Prow, and Makoto Taomoto. We also wish to thank Advanced Biological Research and Stem-X, who provided eyes, for their dedication in assuring that human fetuses are used to advance our knowledge of human development. This work was supported by NIH grants EY01765 (Wilmer) and RO1-EY09357 (GAL), Research to Prevent Blindness (Wilmer), the Himmelfarb Family Foundation, and a Research to Prevent Blindness Senior Scientific Investigator award (GAL).

## References

- Allende A, Madigan MC, Provis JM. Endothelial cell proliferation in the choriocapillaris during human retinal differentiation. *Br J Ophthalmol*. 2006; 90:1046–1051. [PubMed: 16613918]
- Ashton N. Retinal angiogenesis in the human embryo. *Br Med Bull*. 1970; 26:103–106. [PubMed: 4911762]
- Baba T, Grebe R, Hasegawa T, Bhutto I, Merges C, McLeod DS, Lutty GA. Maturation of the fetal human choriocapillaris. *Invest Ophthalmol Vis Sci*. 2009; 50:3503–3511. [PubMed: 19264887]

- Baba T, McLeod DM, Edwards MM, Merges C, Sen T, Sinha D, Lutty GA. VEGF<sub>165b</sub> in the developing vasculatures of the fetal human eye. *Dev Dyn*. 2012; 241:595–607. [PubMed: 22275161]
- Balazs EA, Toth LZ, Ozanics V. Cytological studies on the developing vitreous as related to the hyaloid vessel system. *Albr Von Graefes Arch Klin Exp Ophthalmol*. 1980; 213:71–85.
- Chan-Ling T, McLeod DS, Hughes S, Baxter L, Chu Y, Hasegawa T, Lutty GA. Astrocyte-endothelial cell relationships during human retinal vascular development. *Invest Ophthalmol Vis Sci*. 2004; 45:2020–2032. [PubMed: 15161871]
- Chen T, Bai H, Shao Y, Arzigian M, Janzen V, Attar E, Xie Y, Scadden DT, Wang ZZ. Stromal cell-derived factor-1/CXCR4 signaling modifies the capillary-like organization of human embryonic stem cell-derived endothelium in vitro. *Stem Cells*. 2007; 25:392–401. [PubMed: 17038674]
- Chu Y, Hughes S, Chan-Ling T. Differentiation and migration of astrocyte precursor cells and astrocytes in human fetal retina: relevance to optic nerve coloboma. *FASEB J*. 2001; 15:2013–2015. [PubMed: 11511521]
- Drake CJ, Fleming PA. Vasculogenesis in the day 6.5 to 9.5 mouse embryo. *Blood*. 2000; 95:1571–1579.
- Dubis AM, Costakos DM, Subramaniam CD, Godara P, Wirostko WJ, Carroll J, Provis JM. Evaluation of normal human foveal development using optical coherence tomography and histologic examination. *Arch Ophthalmol*. 2012; 130:1291–1300. [PubMed: 23044942]
- Eichmann A, Corbel C, Nataf V, Vaigot P, Breant C, Le Douarin NM. Ligand-dependent development of the endothelial and hemopoietic lineages from embryonic mesodermal cells expressing vascular endothelial growth factor receptor 2. *Proc Natl Acad Sci U S A*. 1997; 94:5141–5146. [PubMed: 9144204]
- Fruttiger M. Development of the mouse retinal vasculature: angiogenesis versus vasculogenesis. *Invest Ophthalmol Vis Sci*. 2002; 43:522–527. [PubMed: 11818400]
- Hasegawa T, McLeod DS, Bhutto IA, Prow T, Merges CA, Grebe R, Lutty GA. The embryonic human choriocapillaris develops by hemo-vasculogenesis. *Dev Dyn*. 2007; 236:2089–2100. [PubMed: 17654716]
- Hasegawa T, McLeod DS, Prow T, Merges C, Grebe R, Lutty GA. Vascular precursors in developing human retina. *Investigative ophthalmology & visual science*. 2008; 49:2178–2192. [PubMed: 18436851]
- Hellstrom M, Phng LK, Hofmann JJ, Wallgard E, Coultas L, Lindblom P, Alva J, Nilsson AK, Karlsson L, Gaiano N, Yoon K, Rossant J, Iruela-Arispe ML, Kalen M, Gerhardt H, Betsholtz C. Dll4 signalling through Notch1 regulates formation of tip cells during angiogenesis. *Nature*. 2007; 445:776–780. [PubMed: 17259973]
- Hendrickson AE, Yuodelis C. The morphological development of the human fovea. *Ophthalmology*. 1984; 91:603–612. [PubMed: 6462623]
- Hughes S, Yang H, Chan-Ling T. Vascularization of the human fetal retina: roles of vasculogenesis and angiogenesis. *Invest Ophthalmol Vis Sci*. 2000; 41:1217–1228. [PubMed: 10752963]
- Jakobiec FA. *Ocular Anatomy, Embryology, and Teratology*. Harper and Row Publishers, Inc.; Philadelphia, PA: 1982.
- Kawakami Y, Ii M, Matsumoto T, Kuroda R, Kuroda T, Kwon SM, Kawamoto A, Akimaru H, Mifune Y, Shoji T, Fukui T, Kurosaka M, Asahara T. SDF-1/CXCR4 axis in Tie2-lineage cells including endothelial progenitor cells contributes to bone fracture healing. *J Bone Miner Res Off J Am Soc Bone Miner Res*. 2015; 30:95–105.
- Kozulin P, Natoli R, Bumsted O'Brien KM, Madigan MC, Provis JM. The cellular expression of antiangiogenic factors in fetal primate macula. *Invest Ophthalmol Vis Sci*. 2010; 51:4298–4306. [PubMed: 20357200]
- Kozulin P, Natoli R, Madigan MC, O'Brien KM, Provis JM. Gradients of Eph-A6 expression in primate retina suggest roles in both vascular and axon guidance. *Mol Vis*. 2009a; 15:2649–2662. [PubMed: 20011078]
- Kozulin P, Natoli R, O'Brien KM, Madigan MC, Provis JM. Differential expression of anti-angiogenic factors and guidance genes in the developing macula. *Mol Vis*. 2009b; 15:45–59. [PubMed: 19145251]

- Lang RA, Lustig M, Francois F, Sellinger M, Plesken H. Apoptosis during macrophage-dependent ocular tissue remodeling. *Development*. 1994; 120:3395–3403. [PubMed: 7821211]
- Lang RA, Bishop JM. Macrophages are required for cell death and tissue re-modeling in the developing mouse eye. *Cell*. 1993; 74:453–462. [PubMed: 8348612]
- Larrivee B, Freitas C, Suchting S, Brunet I, Eichmann A. Guidance of vascular development: lessons from the nervous system. *Circ Res*. 2009; 104:428–441. [PubMed: 19246687]
- Lundkvist J, Lendahl U. Notch and the birth of glial cells. *Trends Neurosci*. 2001; 24:492–494. [PubMed: 11506867]
- Lutty GA, McLeod DS. Increased retinal glial expression of GFAP and 5' nucleotidase in response to hyperoxia. *Invest Ophthalmol Vis Sci*. 1987; 28:204.
- Mann, IC. *The Development of the Human Eye*. University Press; Cambridge: 1928.
- Marnaros AG, Fan J, Yokoyama Y, Gerber HP, Ferrara N, Crouch RK, Olsen BR. Vascular endothelial growth factor expression in the retinal pigment epithelium is essential for choriocapillaris development and visual function. *Am J Pathol*. 2005; 167:1451–1459. [PubMed: 16251428]
- McLeod DS, Hasegawa T, Baba T, Grebe R, Galtier d'Auriac I, Merges C, Edwards M, Lutty GA. From blood islands to blood vessels: morphologic observations and expression of key molecules during hyaloid vascular system development. *Invest Ophthalmol Vis Sci*. 2012; 53:7912–7927. [PubMed: 23092923]
- McLeod DS, Hasegawa T, Prow T, Merges C, Lutty G. The initial fetal human retinal vasculature develops by vasculogenesis. *Dev Dyn*. 2006; 235:3336–3347. [PubMed: 17061263]
- McLeod DS, Lutty GA. High resolution histologic analysis of the human choroidal vasculature. *Invest Ophthalmol Vis Sci*. 1994; 35:3799–3811. [PubMed: 7928177]
- McLeod DS, Lutty GA, Wajer SD, Flower RW. Visualization of a developing vasculature. *Microvasc Res*. 1987; 33:257–269. [PubMed: 2438539]
- Michaelson IC. The mode of development of the vascular system of the retina, with some observations on its significance for certain retinal diseases. *Trans Ophthalmol Soc UK*. 1948; 68:137–180.
- Noronha-Matos JB, Costa MA, Magalhaes-Cardoso MT, Ferreirinha F, Pelletier J, Freitas R, Neves JM, Sevigny J, Correia-de-Sa P. Role of ecto-NTPDases on UDP-sensitive P2Y(6) receptor activation during osteogenic differentiation of primary bone marrow stromal cells from postmenopausal women. *J Cell Physiol*. 2012; 227:2694–2709. [PubMed: 21898410]
- Oguni M, Tanaka O, Shinohara H, Yoshioka T, Setogawa T. Ultrastructural study on the retinal pigment epithelium of human embryos, with special reference to quantitative study on the development of melanin granules. *Acta Anat*. 1991; 140:335–342. [PubMed: 1927245]
- Outtz HH, Tattersall IW, Kofler NM, Steinbach N, Kitajewski J. Notch1 controls macrophage recruitment and Notch signaling is activated at sites of endothelial cell anastomosis during retinal angiogenesis in mice. *Blood*. 2011; 118:3436–3439. [PubMed: 21795743]
- Perlingeiro RC. Endoglin is required for hemangioblast and early hematopoietic development. *Development*. 2007; 134:3041–3048. [PubMed: 17634194]
- Provis JM, Hendrickson AE. The foveal avascular region of developing human retina. *Arch Ophthalmol*. 2008; 126:507–511. [PubMed: 18413520]
- Provis JM, Leech J, Diaz C, Penfold PL, Stone J, Keshet E. Development of the human retinal vasculature: cellular relations and VEGF expression. *Exp Eye Res*. 1997; 65:555–568. [PubMed: 9464188]
- Provis JM, Sandercoe T, Hendrickson AE. Astrocytes and blood vessels define the foveal rim during primate retinal development. *Invest Ophthalmol Vis Sci*. 2000; 41:2827–2836. [PubMed: 10967034]
- Roca C, RH A. Regulation of vascular morphogenesis by Notch signaling. *Genes Dev*. 2007; 21:2511–2524. [PubMed: 17938237]
- Saint-Geniez M, Maldonado AE, D'Amore PA. VEGF expression and receptor activation in the choroid during development and in the adult. *Invest Ophthalmol Vis Sci*. 2006; 47:3135–3142. [PubMed: 16799060]
- Sandercoe TM, Madigan MC, Billson FA, Penfold PL, Provis JM. Astrocyte proliferation during development of the human retinal vasculature. *Exp Eye Res*. 1999; 69:511–523. [PubMed: 10548471]

- Sequeira Lopez ML, Chernavsky DR, Nomasa T, Wall L, Yanagisawa M, Gomez RA. The embryo makes red blood cell progenitors in every tissue simultaneously with blood vessel morphogenesis. *Am J Physiol Regul Integr Comp Physiol.* 2003; 284:R1126–R1137. [PubMed: 12626371]
- Taomoto M, McLeod DS, Merges C, Lutty GA. Localization of adenosine A2a receptor in retinal development and oxygen-induced retinopathy. *Invest Ophthalmol Vis Sci.* 2000; 41:230–243. [PubMed: 10634625]
- Wang L, Guo S, Zhang N, Tao Y, Zhang H, Qi T, Liang F, Huang Z. The role of SDF-1/CXCR4 in the vasculogenesis and remodeling of cerebral arteriovenous malformation. *Ther Clin Risk Manag.* 2015; 11:1337–1344. [PubMed: 26366086]
- Xu Q, Wang Y, Dabdoub A, Smallwood PM, Williams J, Woods C, Kelley MW, Jiang L, Tasman W, Zhang K, Nathans J. Vascular development in the retina and inner ear: control by Norrin and Frizzled-4, a high-affinity ligand-receptor pair. *Cell.* 2004; 116:883–895. [PubMed: 15035989]
- Zhu M, Madigan MC, van Driel D, Maslim J, Billson FA, Provis JM, Penfold PL. The human hyaloid system: cell death and vascular regression. *Exp Eye Res.* 2000; 70:767–776. [PubMed: 10843781]
- Zhu M, Provis JM, Penfold PL. The human hyaloid system: cellular phenotypes and inter-relationships. *Exp Eye Res.* 1999; 68:553–563. [PubMed: 10328969]

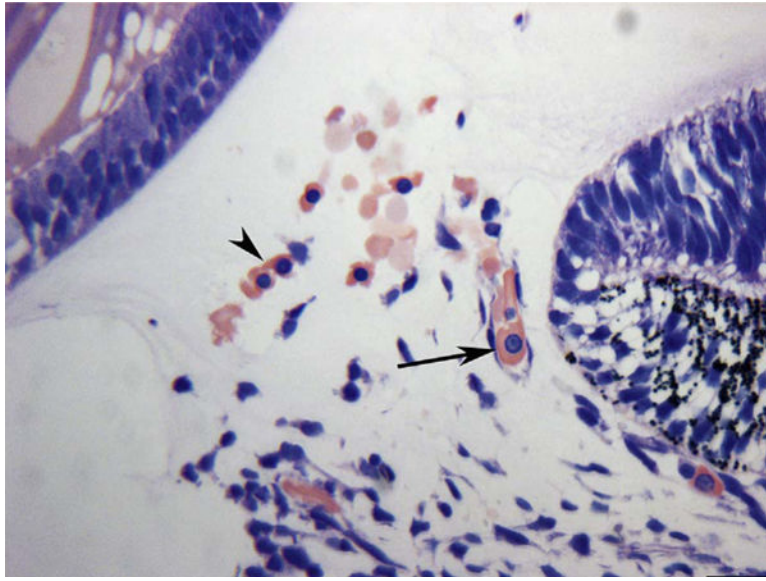


**Fig. 1.** Anlage of mesenchymal cells in the annular opening at the pupillary margin in a 5.5-week gestation (WG) human eye. Note the free erythroblasts (arrowhead, acidophilic cytoplasm with a prominent nucleus) and an erythroblast in a developing blood vessel (arrow). (Wright's Giemsa) Scale Bar = 20  $\mu$ m.

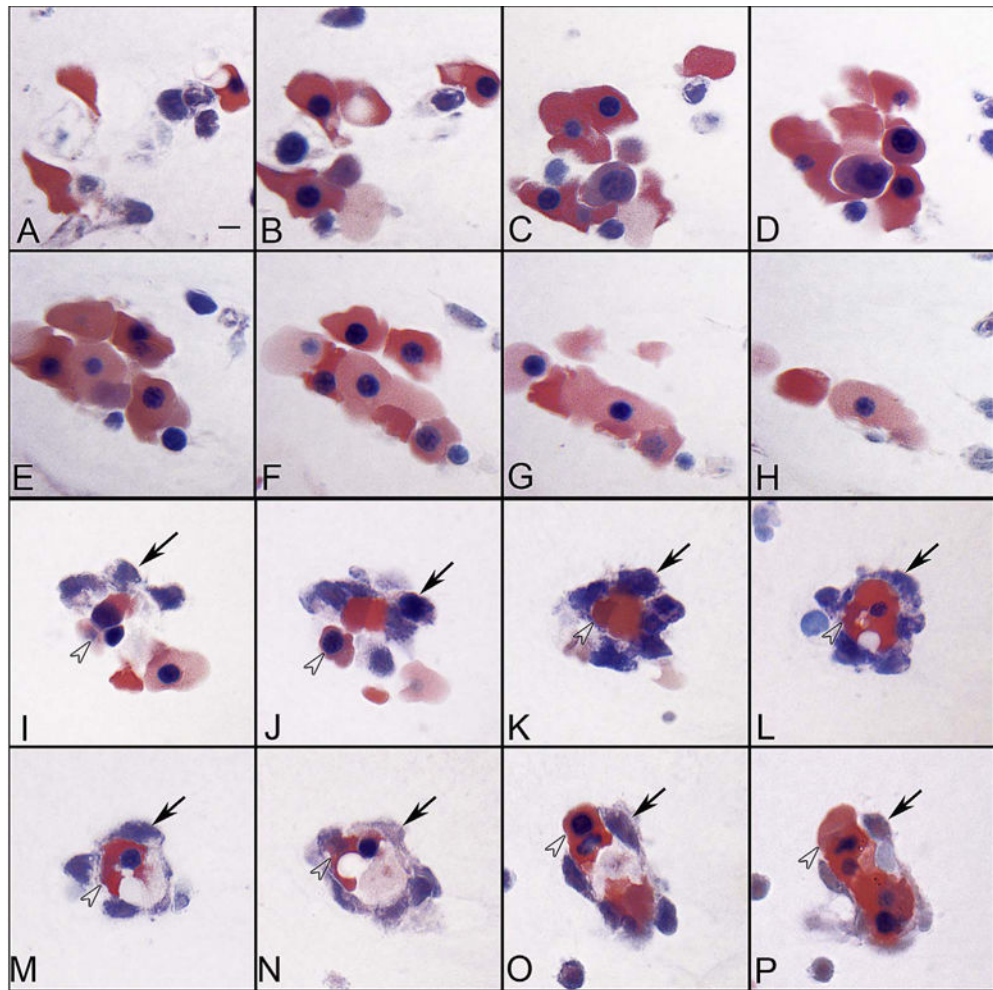


**Fig. 2.** Blood island-like structures in serial sections of the vitreous at 5.5 WG. Some island-like structures are aggregates of erythroblasts (A–H), while others were composed of basophilic mesenchyme (arrows) (I–P) around a core of acidophilic erythroblasts (arrowheads). (Wrights-Giemsa stain, Scale bar in A = 10  $\mu$ m for all) (Fig. 2 from McLeod et al., *Invest. Ophthalmol. Vis. Sci.* 53:7915, 2012, with permission).

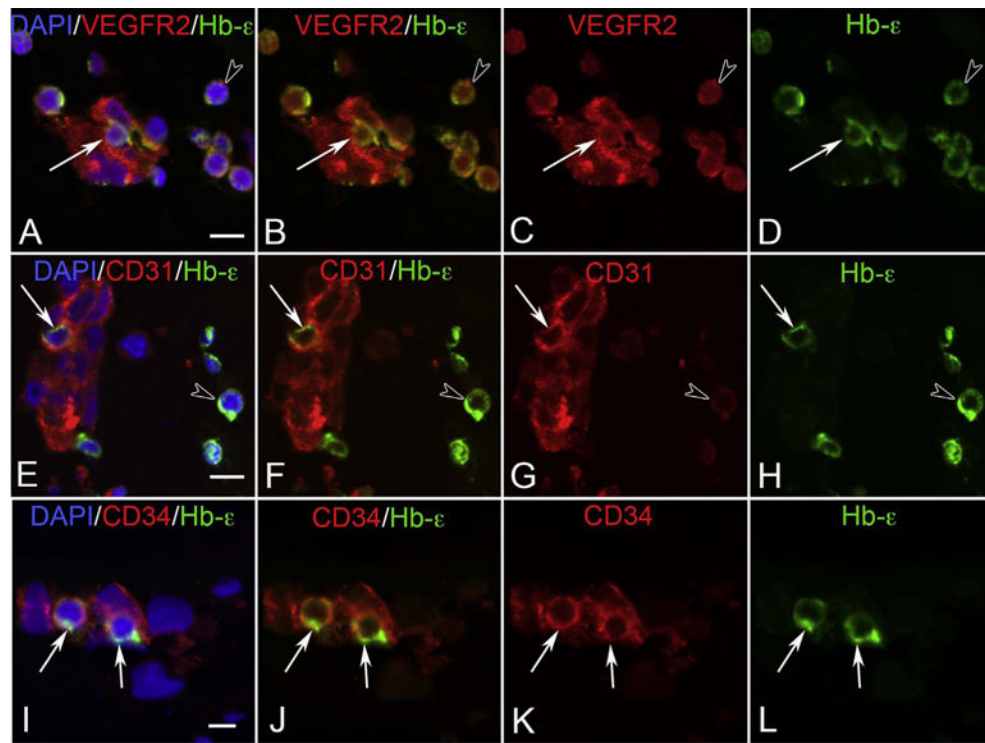


**Fig. 3.** VEGFR2 (A–D), CD31 (E–H) and CD34 (I–L) labeling (all red) with epsilon hemoglobin (green, Hb- $\epsilon$ ) and DAPI (blue, nuclei) in blood island-like structures in the 6 WG vitreous. Free erythroblasts co-expressed VEGFR2 and Hb- $\epsilon$  (arrowhead in A–D) as did some cells within blood islands (arrow in A–D). All cells of the blood islands expressed VEGFR2. CD31 and Hb- $\epsilon$  were co-expressed in select cells of blood islands (arrow in E–H) while free Hb- $\epsilon^+$  erythroblasts were only weakly immunoreactive for CD31 (arrowhead in E–H). CD34 and Hb- $\epsilon$  were co-expressed in some scattered cells in blood island-like structures (arrows in I–L), while free Hb- $\epsilon^+$  erythroblasts were CD34 $^-$  (not shown). (Scale bar in A, E & I = 10  $\mu$ m) (Fig. 5 from McLeod et al., *Invest. Ophthalmol. Vis. Sci.* 53:7918, 2012, with permission).

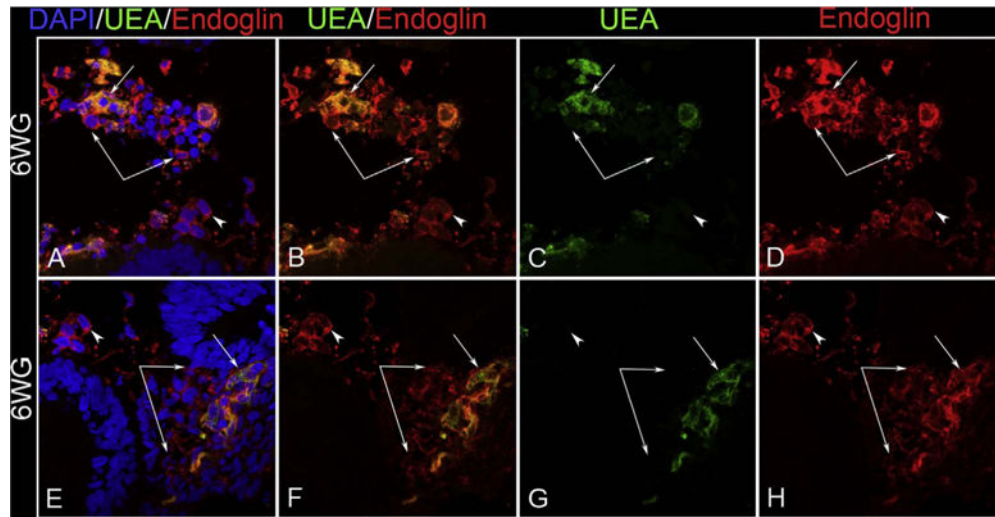


**Fig. 4.** Localization of endoglin (red) and Ulex europaeus lectin (green) at the pupillary margin at 6 WG. Most cells in the mesenchymal anlage express endoglin but some also co-express UEA, a marker for human endothelial cells. (Scale Bar = 20  $\mu$ m).

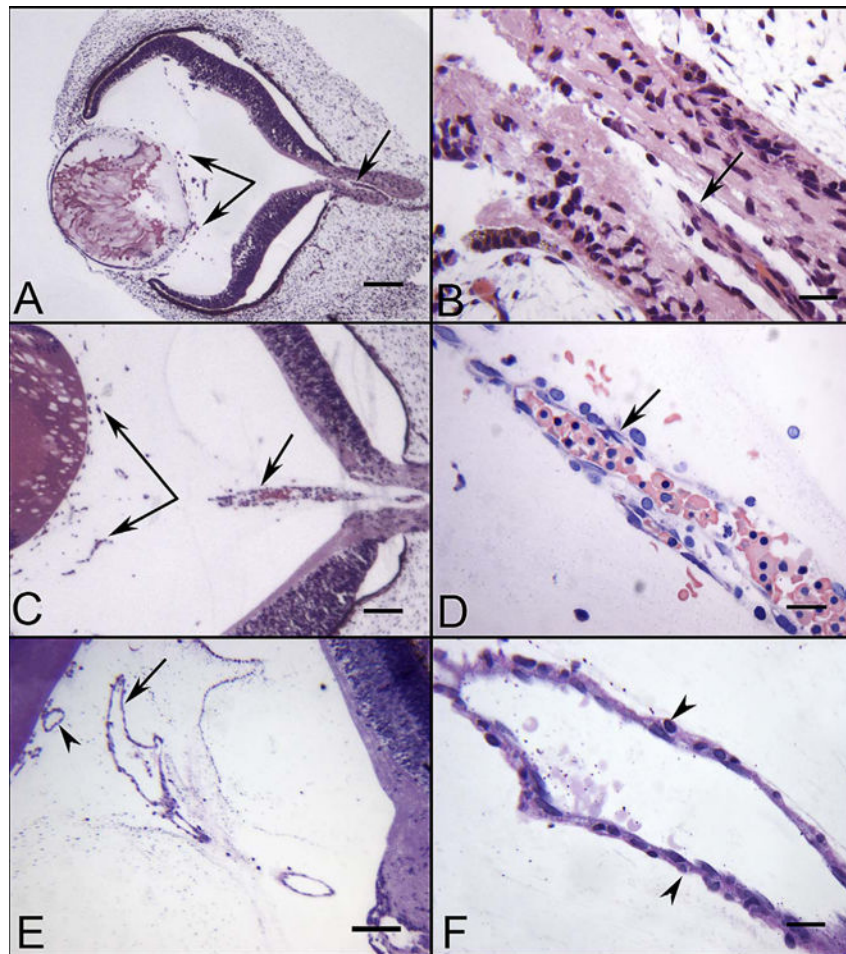


**Fig. 5.** Glycol methacrylate (JB-4) sections of eyes at 5.5 (A–B), 7 (C–D) and 12 WG (E–F) showing the blood vessels in vitreous and the hyaloid artery. The hyaloid artery at 5.5 WG had not penetrated the vitreous cavity but was present in the optic stalk (arrow in A & B). Near the lens vesicle, blood island-like structures were formed in vitreous cavity (paired arrows in A). The hyaloid artery at 7 WG had invaded the vitreous and contained packed erythroblasts (arrow in C & D). Blood vessels were present near the lens in the vitreous and on the surface of the lens (paired arrows in C). The hyaloid artery was fully formed by 12 WG and had several major branches near the posterior surface of the lens (arrow in E). The outer wall of the hyaloid artery had smooth muscle cells (arrowheads in F). (A–C hematoxylin & eosin stain, D Wrights-Giemsa stain, E & F Periodic acid-Schiff and hematoxylin stain, Scale bars = 100  $\mu$ m in A,C & E, 20  $\mu$ m in B,D & F) (Fig. 1 from McLeod et al., *Invest. Ophthalmol. Vis. Sci.* 53:7918, 2012, with permission).

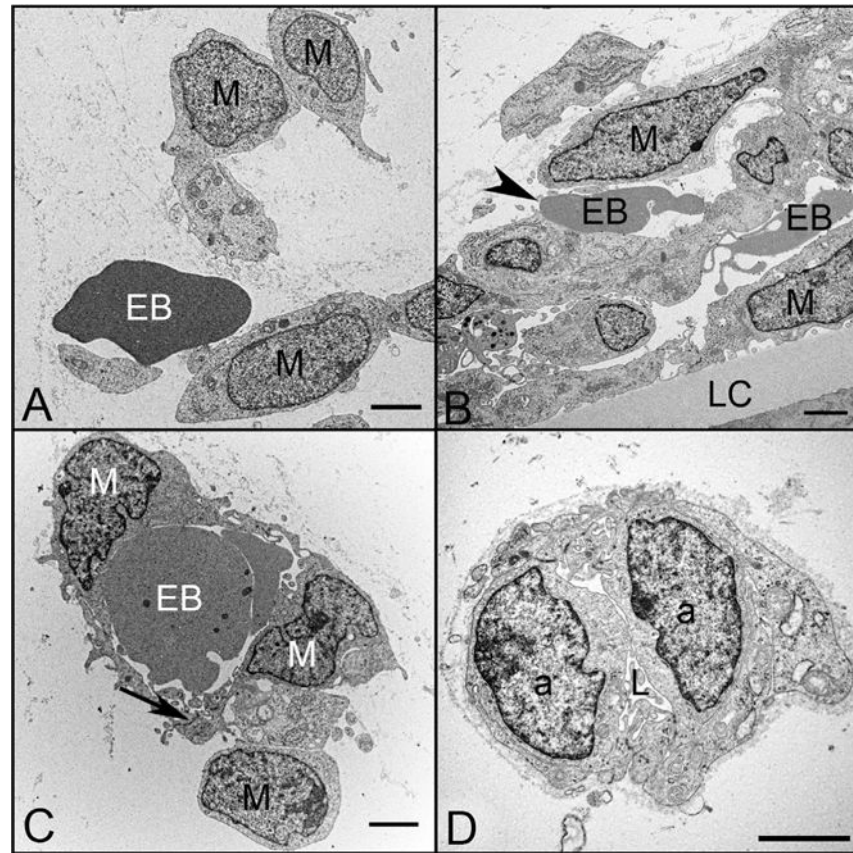


**Fig. 6.** Ultrastructural features of blood island-like structures (A–C) and angioblastic aggregates (D) in the vitreous of a 6.5 WG embryonic eye. Angioblasts (a), erythroblasts (EB), mesenchymal cells (M), and early lumen formation (L) were present at this age. Blood island-like structures (A–C) were composed of loosely arranged mesenchymal cells with free erythroblasts (A), incompletely enveloped erythroblasts (arrowhead) (B), and erythroblasts completely enveloped by mesenchymal cells (C). Angioblastic aggregates (a) initially formed cords (D) with slit-like lumens (L). There was a paucity of basement membrane material surrounding these blood islands and primitive capillaries. (Scale bars = 2  $\mu$ m in all).

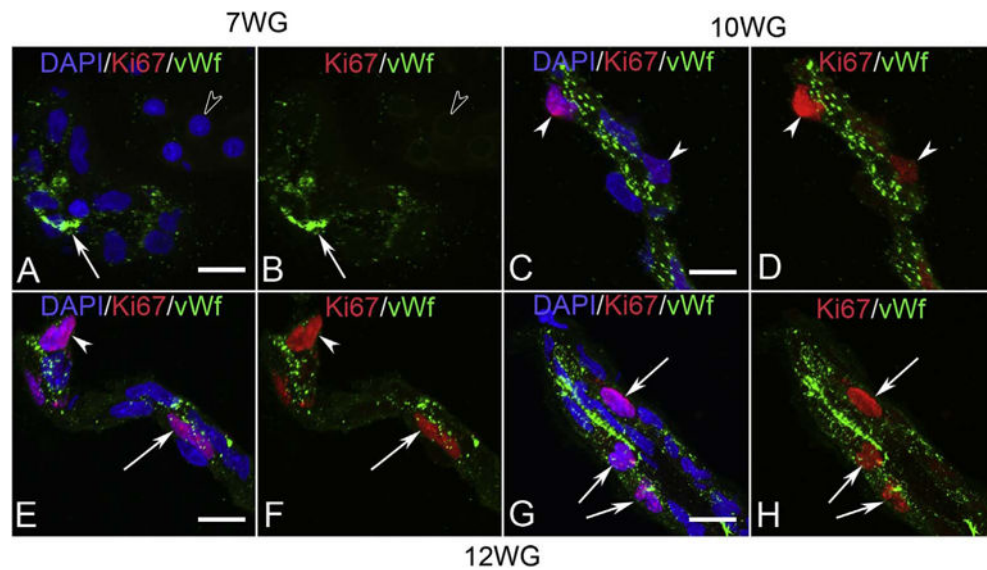


**Fig. 7.** Ki67 (red) and von Willibrand factor (vWf) (green) labeling in blood island-like structures of vitreous at 7 WG (A & B) and blood vessels at 10 WG (C & D) and 12 WG (E–H). Free erythroblasts did not label for vWf (open arrowhead in A & B) at 7 WG but some blood island cells expressed vWf (arrow). No Ki67 labeling was observed in nuclei of cells within the vitreous at this age. vWf immunoreactivity at 10 WG was prominent in endothelial cells and some cells had Ki67 labeled nuclei. These cells were primarily on the outer capillary wall in a pericyte position (arrowheads in C & D). Occasional endothelial cells (arrow) and pericytes (arrowhead) of capillaries (E & F) at 12 WG were proliferating as were endothelial cells in the hyaloid artery (arrows in G & H). (Scale bar in A, C, E & F = 10  $\mu$ m) (Fig. 11 from McLeod et al., *Invest. Ophthalmol. Vis. Sci.* 53:7925, 2012, with permission).

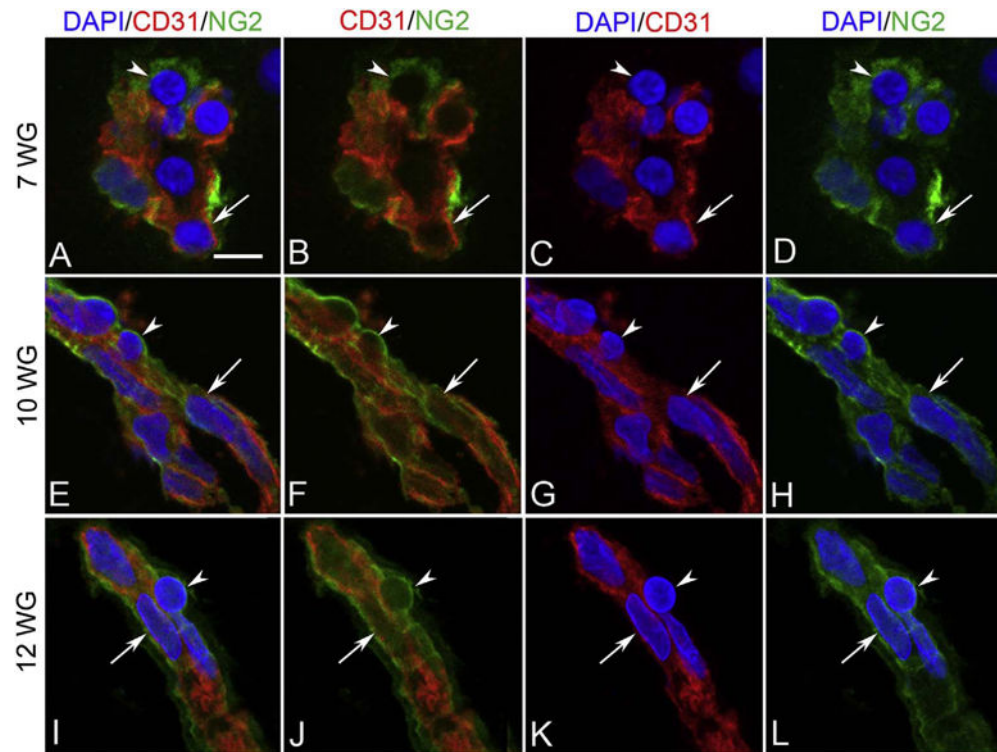


**Fig. 8.** NG-2 (green) and CD31 (red) labeling in blood island-like structures at 7 WG in vitreous (A–D), and at 10 WG (E–H) and 12 WG (I–L) in blood vessels. Some blood island cells at 7 WG were CD31<sup>+</sup>/NG-2<sup>+</sup> (arrow in A–D) and others were CD31<sup>-</sup>/NG-2<sup>+</sup> (arrowhead in A–D). Blood vessels at 10 and 12 WG had CD31<sup>+</sup> endothelial cells (arrow in E–H) and CD31<sup>-</sup> pericytes (arrowhead in E–H) and were immunoreactive for NG-2. (Scale bar in A = 10  $\mu$ m for all) (Fig. 9 from McLeod et al., *Invest. Ophthalmol. Vis. Sci.* 53:7923, 2012, with permission).

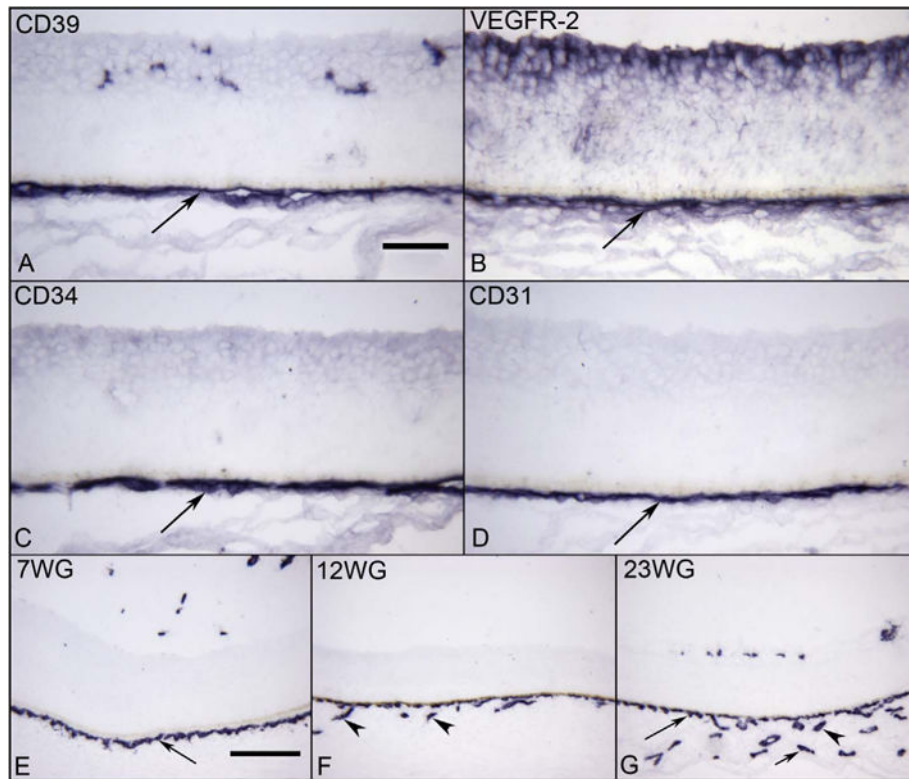


**Fig. 9.** Vascular markers in choroid at 6 WG (A–D) and CD34 labeling at different ages (E–G). A layer of CD39<sup>+</sup> (A), VEGFR-2<sup>+</sup> (B), CD34<sup>+</sup> (C), and CD31<sup>+</sup> (D) cells represents the forming choriocapillaris (CC) (arrows) at 6 WG. The angioblasts in retina also express VEGFR-2 (top in B). At 7 WG, CD34 is expressed only by forming CC layer (arrow) and it is not until 12 WG (F) that the intermediate CD34<sup>+</sup> blood vessels in Sattler's layer are present (arrowhead). By 23 WG, all three layers of CD34<sup>+</sup> choroidal blood vessels are present (G) (CC, long arrow, Sattler's arrowhead, and Haller's short arrow). The RPE cells are present above the CC in all plates, but the pigment has been bleached. (APase all; Scale bar = 50  $\mu$ m in A–D, 100  $\mu$ m in E–G).

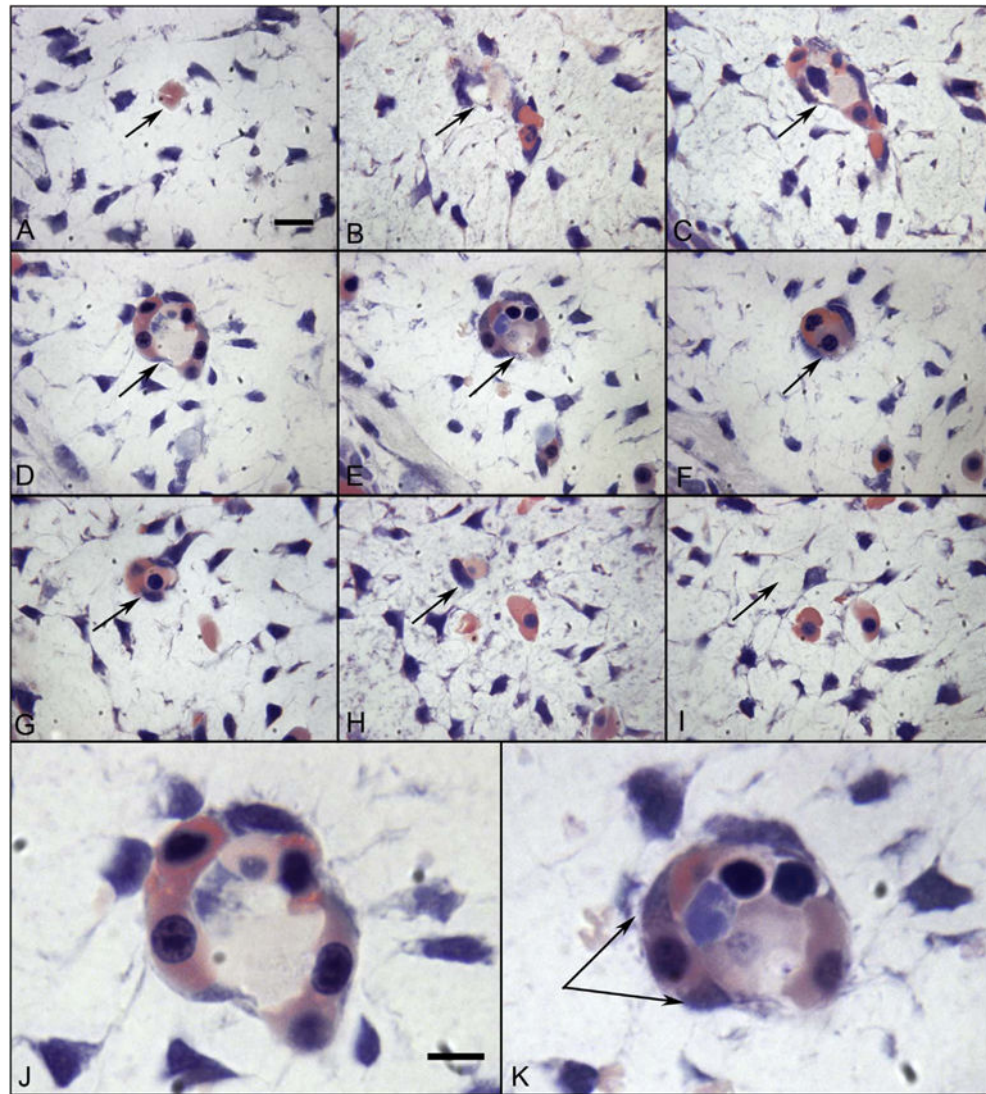


**Fig. 10.** Glycol methacrylate (JB4) sections showing a blood island-like structure in the choroid at 6 WG. Serial sections (A–I) confirm that the structure is isolated and separated from any blood vessels. The same position in each panel is indicated by an arrow. High magnification photos of D and E are shown in J and K respectively. Wright’s Giemsa stain demonstrates acidophilic cytoplasm in many cells, which is indicative of hemoglobin (pink) and nuclei are basophilic (blue). One cell outside of structure (double arrow in K) has cytoplasmic staining pattern that appears to be turning from acidophilic into basophilic, which suggests that the cell has both the characteristics of hematopoietic cells and endothelial cells. (Wright’s Giemsa; Bar A–I = 10  $\mu$ m, bar J–K = 10  $\mu$ m) (Fig. 2 from Hasegawa et al., *Developmental Dynamics* 236:2091; Fig. 2 from Hasegawa et al., *Developmental Dynamics* 236:2007, with permission).

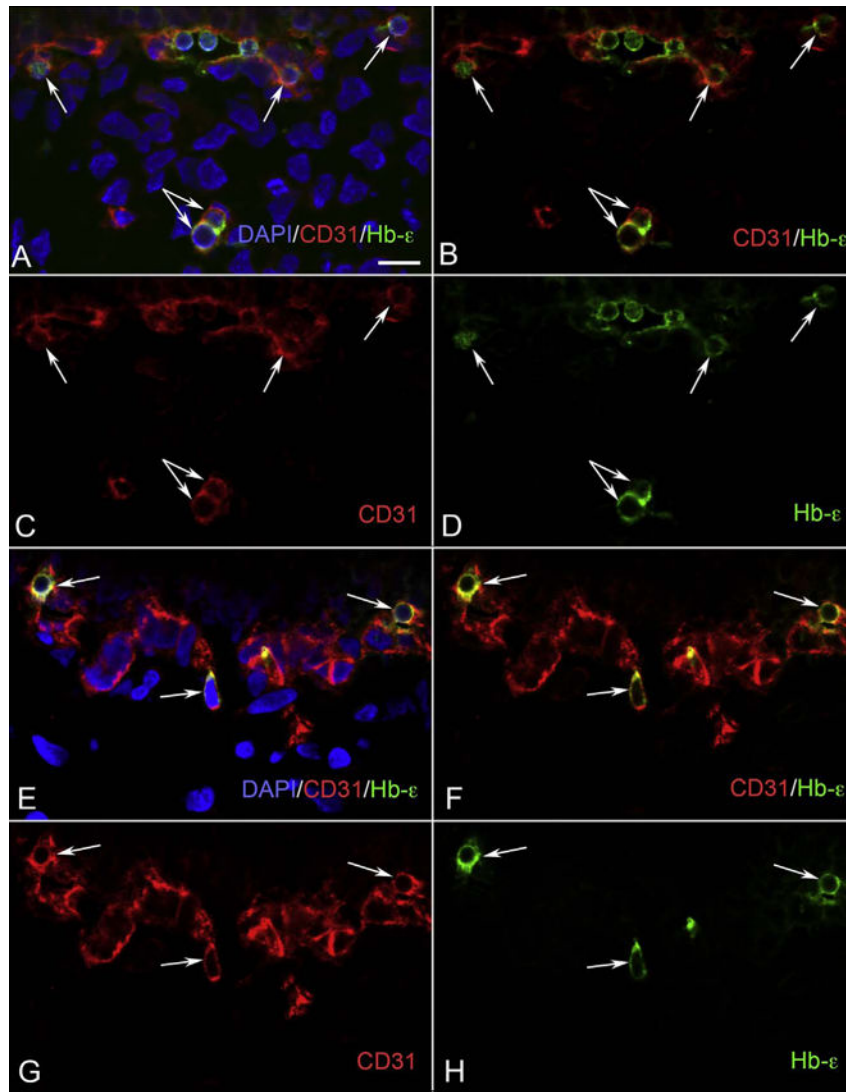


**Fig. 11.** CD31/Hb- $\epsilon$  double positive cells in developing choroid. (A–D) Clusters of CD31<sup>+</sup>/Hb- $\epsilon$ <sup>+</sup> (red/green) (arrows) were visible in the choriocapillaris layer at 6 WG, whereas in the choroidal stroma had isolated cells (double arrow) that were also double positive. (E–H) There were isolated cells (arrows) that were CD31/Hb- $\epsilon$  positive at 7 WG, which appeared to be attached to the choriocapillaris. Some of these cells were deep in the choroid, resembling those found at 6 WG. Having both CD31/Hb- $\epsilon$  positive in the same cells gives them characteristics of hematopoietic and endothelial cells. B and F are merged images of the single color images C, D and G, H, respectively. A and E are images showing nuclear counter staining with DAPI (blue) merged with B and F, respectively. (Scale bar = 10  $\mu$ m) (Fig. 4 from Hasegawa et al., *Developmental Dynamics* 236:2093 Fig. 4 from Hasegawa et al., *Developmental Dynamics* 236:2007, with permission).

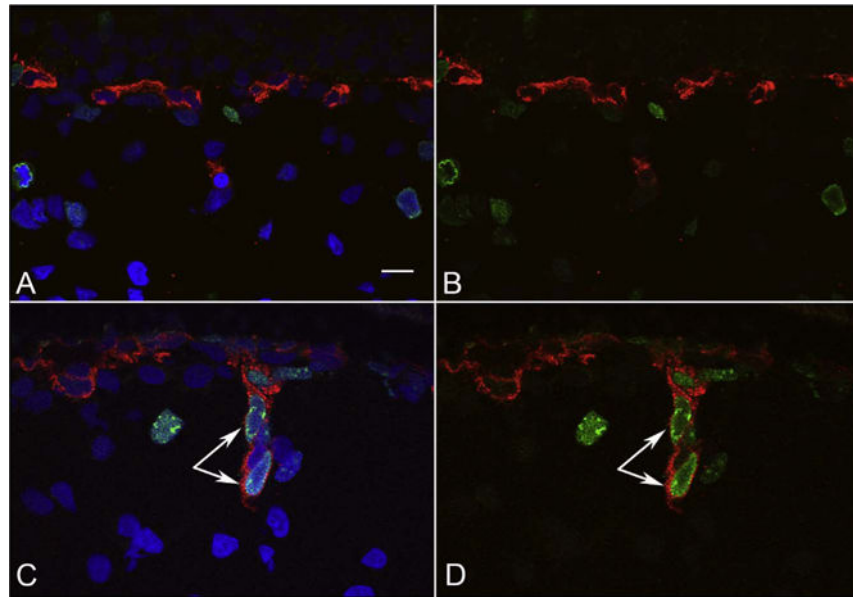


**Fig. 12.** CD34/Ki67 staining of fetal choroid. There are no CD34 (red) and Ki67 (green) double stained cells at 6 WG (A, B), while CD34/Ki67 double positive cells (arrow) were observed in a forming intermediate vessel at 12 WG (C, D). B and D are merged images of CD34 (Red) and Ki67 (Green). A and C are merged B and D with DAPI nuclear counterstaining (blue). (Bar = 10  $\mu$ m) (Fig. 8 from Hasegawa et al., *Developmental Dynamics* 236:2096 Fig. 8 from Hasegawa et al., *Developmental Dynamics* 236:2007, with permission).

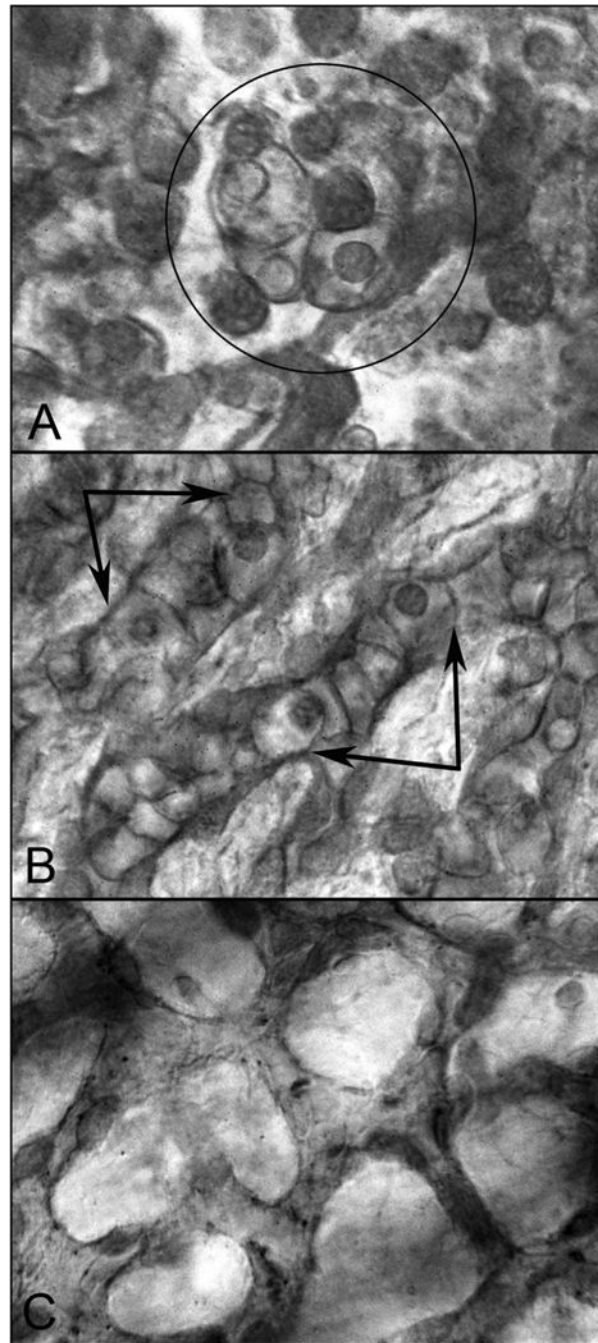


**Fig. 13.** CD39 labeled flat choroids shows the pattern of the developing CC in embryonic and fetal human eyes. (A) CD39<sup>+</sup> cells are organized into blood island-like structures (circle) at 5.5 WG. (B) Highly cellular linear cord-like structures without apparent lumen have formed at 9 WG (double arrows). (C) The capillaries are narrower, lumens have formed, and cellularity has decreased markedly at 12 WG. (Scale bar = 10  $\mu$ m) (Fig. 3 from McLeod and Lutty, Chapter 104, page 1506 in *The New Visual Neurosciences*, Ed. Werner J.S. and Challupa, L.M., MIT Press, 2014).

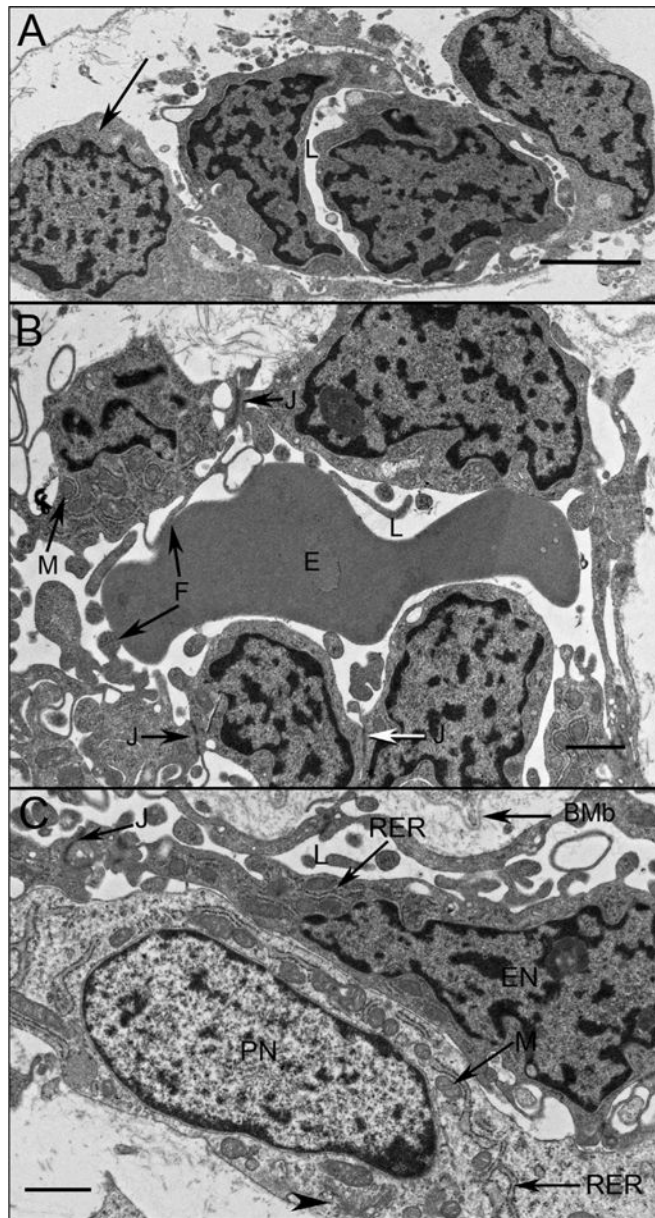


**Fig. 14.** Choriocapillaris ultrastructure at 11 WG in periphery (A), equator (B), and posterior pole (C). Undifferentiated angioblasts (pericyte and endothelial cell precursors) in peripheral choroid had dense chromatin and formed loosely arranged aggregates with slit-like lumens (L). At the equator (B) immature endothelial cells had numerous mitochondria (M) with some tight junctions present (J). Complex membranous infoldings resembling filopodia extended into the developing lumen (F). Immature erythrocytes (E) were present in the lumen and their membranes appeared to fuse with the filopodia. (C) Pericyte-like cells were observed in posterior pole where they appeared more differentiated, with dispersed chromatin in their nuclei (PN) and numerous mitochondria (M) in close proximity with rough endoplasmic reticulum (RER) and Golgi (arrowhead). Endothelial cells had condensed chromatin in their nuclei (EN), made tight junctions with one another (J). In the

posterior pole, Bruch's membrane (BMb) was starting to form posterior to the RPE. (Scale bar in A & B 2  $\mu\text{m}$ , and C 1  $\mu\text{m}$ ) (Fig. 2 from Baba et al., *Invest. Ophthalmol. Vis. Sci.* 50:3506, 2009, with permission).

Author Manuscript

Author Manuscript

Author Manuscript

Author Manuscript

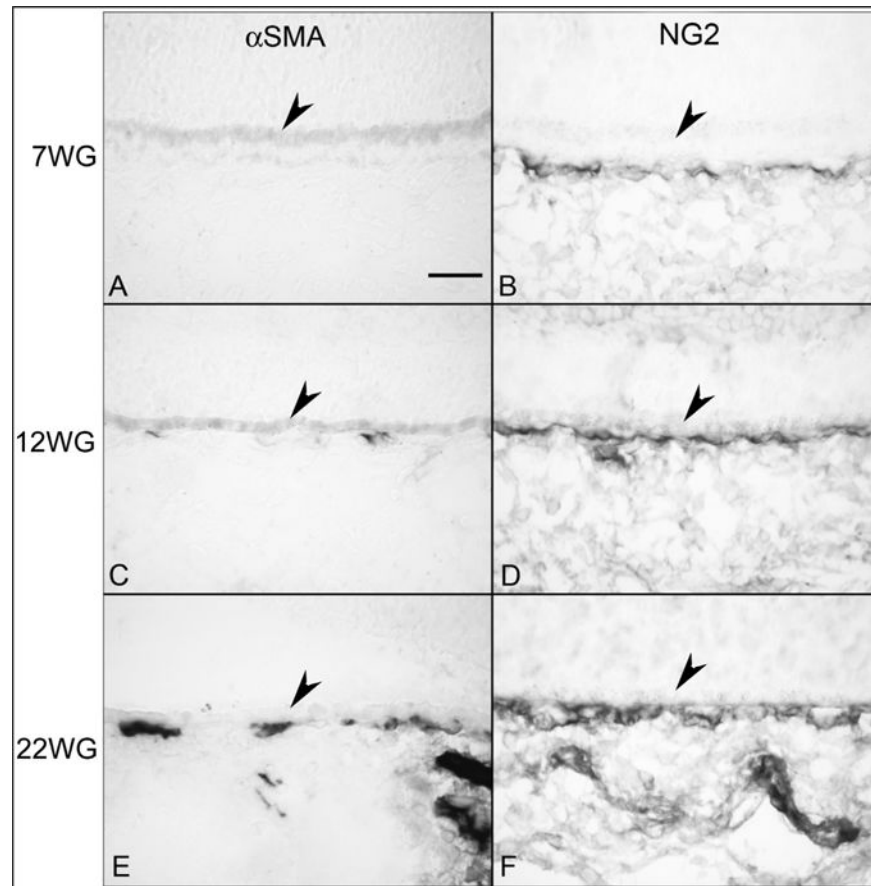


**Fig. 15.**

Alpha smooth muscle actin ( $\alpha$ SMA) (A, C & E) and NG2 labeling (B, D & F) in choroid at 7 (A,B), 12 (C,D) and 22 WG (E,F). No immunoreactivity for  $\alpha$ SMA (A) was observed at 7 WG but NG2 (B) labeled cells were associated with the choriocapillaris. Some scattered  $\alpha$ SMA positive cells (C) were associated with choriocapillaris at 12 WG and NG2 staining (D) was more intense.  $\alpha$ SMA immunoreactivity (E) was associated with choriocapillaris at 22 WG and was present in medium and large choroidal vessels. NG2 labeling was intense in all vessels. (Scale bar = 30  $\mu$ m) (Fig. 6 from Baba et al., *Invest. Ophthalmol. Vis. Sci.* 50:3507, 2009, with permission).

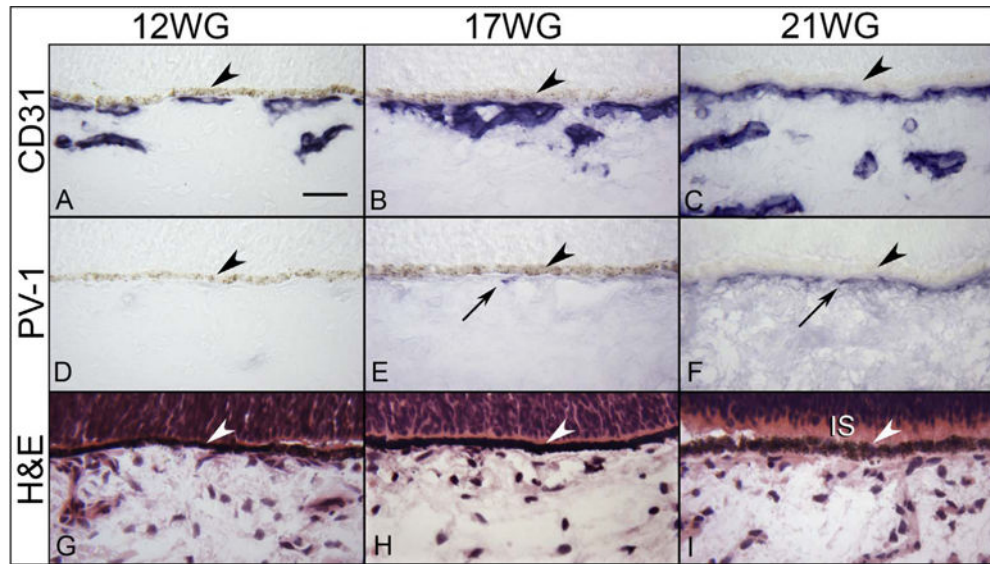


**Fig. 16.** Immunohistochemical localization of CD31 (A–C) and PV-1 (D) in 12 (A,D), 17 WG (B,E), and 21 WG (C,F) choroid. CD31 labels the choriocapillaris and developing intermediate vessels while no PV-1 immunolabeling is seen until 17 WG and more prominently at 21 WG. The structure of the choroid is shown with H & E at the three ages (G–I). Inner segments (IS) are starting to form at 21 WG (I). (arrowhead, RPE; scale bar 30  $\mu$ m; A–F, APase immunoreactivity with bleaching).

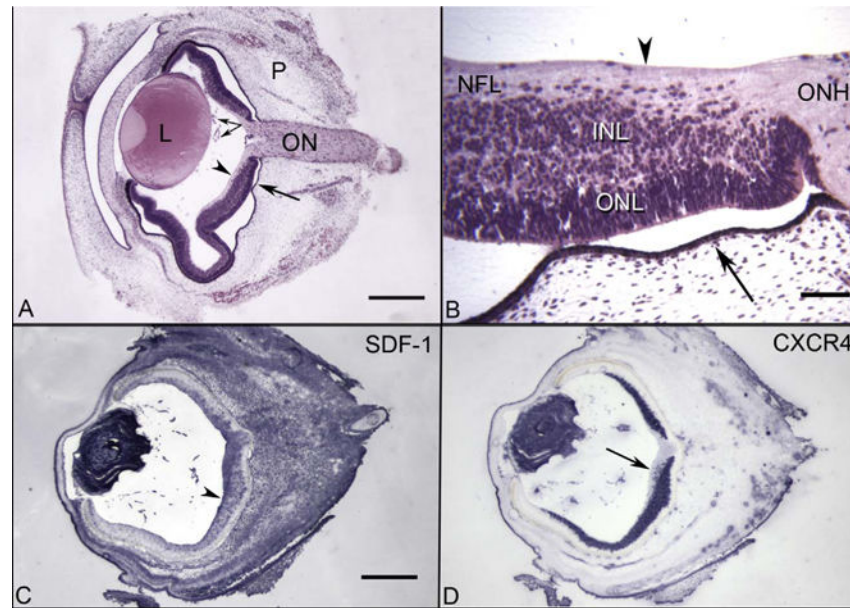


**Fig. 17.**

Cross sections of 7 WG embryonic human eye embedded in JB4 (A–B) and from cryosections that were immunolabeled (C–D). (A) The transient fetal vasculature of the vitreous (paired arrows) is present near the posterior surface of the lens (L). The choriocapillaris (arrow) is developing under the RPE and the optic nerve (ON) is in perfect cross section. The outer layer of the embryonic eye is periocular mesenchyme (P). The internal limiting membrane of retina is indicated by an arrowhead. (B) Higher magnification of the peripapillary region shows the internal limiting membrane (arrowhead), the nerve fiber layer (NFL), the inner neuroblastic layer (INL) the outer neuroblastic layer (ONL) and optic nerve head (ONH). Fusiform-shaped cells appear to be migrating from the INL into the NFL in this region. (C) SDF-1 immunolabeling is intense in the lens, fetal vasculature in vitreous, and a gradient of staining in the NFL (arrowhead) and INL of retina is present, which decreases towards the periphery. SDF-1 immunoreactivity was also intense in the periocular mesenchyme. (D) The adjacent cryosection, which was immunolabeled with anti-CXCR4, demonstrates CXCR4 is present at high levels in the lens, fetal vasculature, and in the neuroblastic layer of retina. Note that the fusiform-shaped cells that appear to be migrating in the NFL are CXCR4<sup>+</sup> (arrow). (A–B hematoxylin and eosin; C–D APase/NBT blue reaction product after bleaching) (Fig. 1 from Hasegawa et al. *Invest. Ophthalmol. Vis. Sci.* 49:2018 Fig. 1 from Hasegawa et al. *Invest. Ophthalmol. Vis. Sci.* 49:2008, with permission).

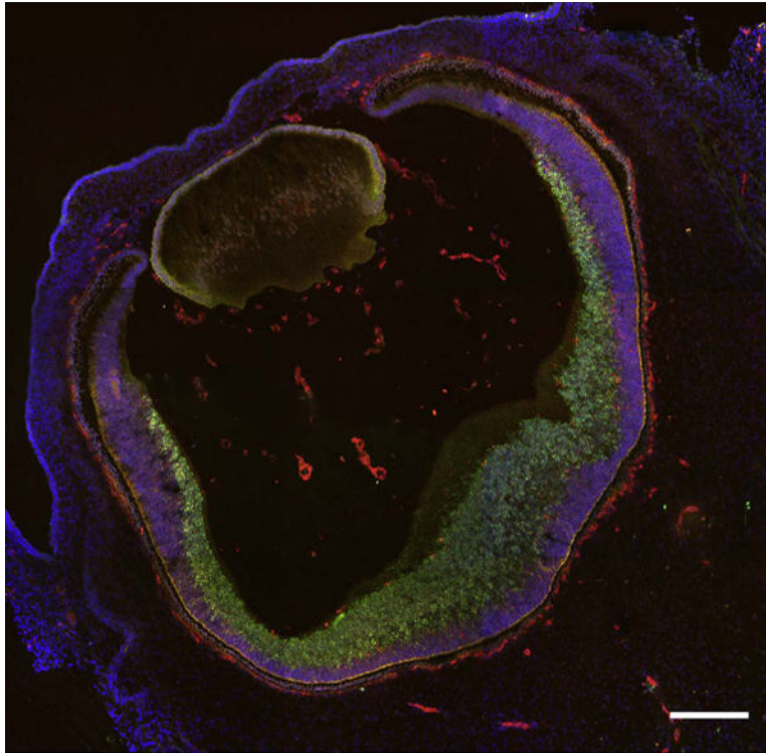


**Fig. 18.** Cryosection of a 7 WG eye immunolabeled with anti-CD39 (red) and anti-CXCR4 (green) and counterstained with DAPI (blue). The fetal vasculature in vitreous and the CC prominently express CD39 as well as angioblasts in inner retina. The inner neuroblastic layer cells, as well as some cells in inner retina, express CXCR4. Scale bar = 50  $\mu$ m.

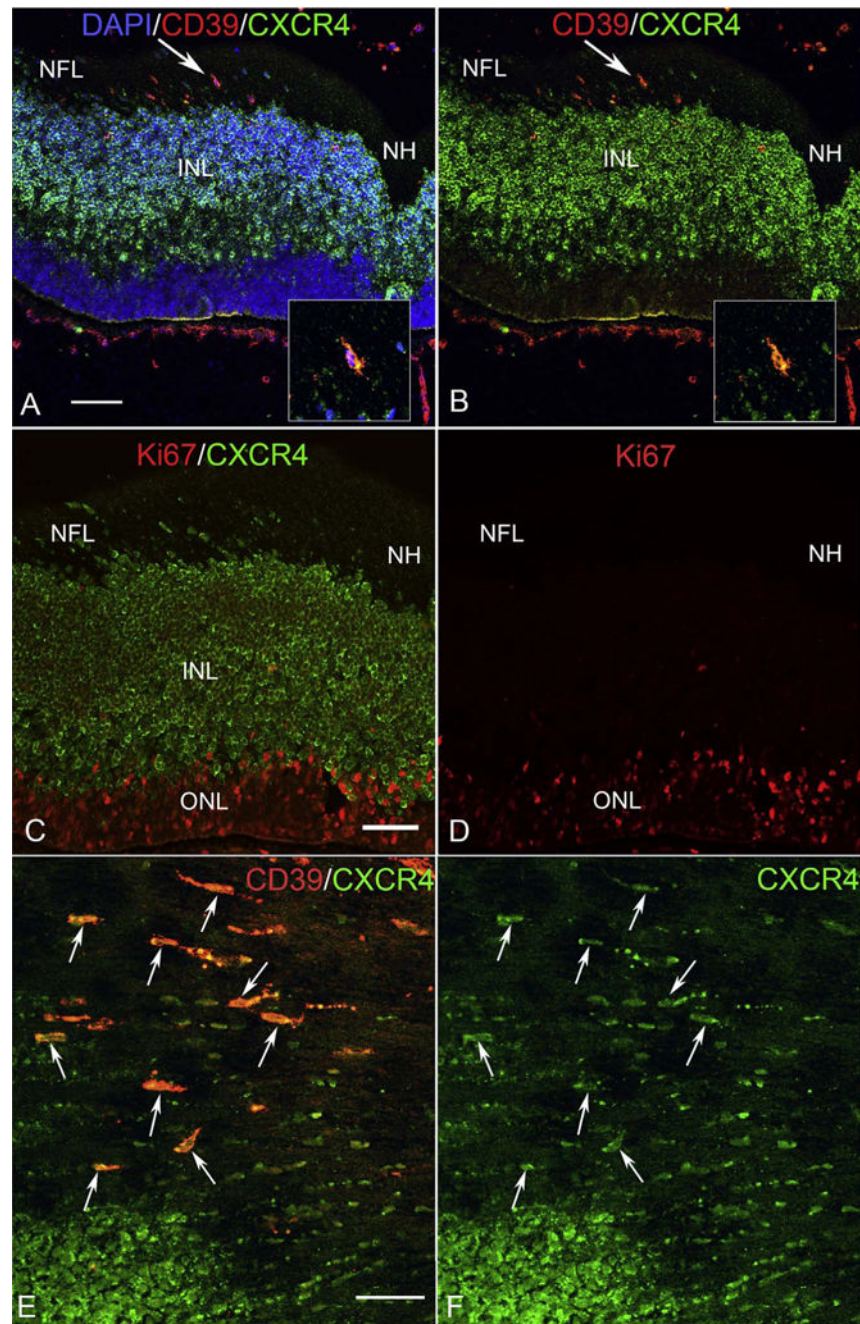


**Fig. 19.** Cryosections (A–D) and a whole mount retina (E–F) from 7 WG eyes. (A) Near the nerve head (NH), fusiform-shaped cells in the nerve fiber layer (NFL) were positive for both CXCR4 (green) and CD39 (red) (arrow in A–B). Inset shows the double-labeled cell indicated by the arrow in “A”–“B” at higher magnification. (DAPI counterstain showing the blue nuclei, red CD39 and green CXCR4 channels) (B) Same section without the DAPI channel shows CXCR4 immunostained cells the entire inner neuroblastic layer and some double-labeled cells in the nerve fiber layer express CXCR4. A few double-labeled cells are near the inner portion of the INL. (C) Same area in a serial section labeled for CXCR4

(green) and Ki67 (red). Only the outer neuroblastic layer is Ki67<sup>+</sup>. (D) Same section with the CXCR4 green channel turned off. (E) Retinal whole mount shows fusiform-shaped cells (arrows) near the optic nerve head (to the right and out of the field) that express both CD39 (red) and CXCR4 (green). (F) Same region as “E” with only the green CXCR4 channel shown. (A–D scale bar = 20  $\mu$ m; E–F scale bar = 40  $\mu$ m).

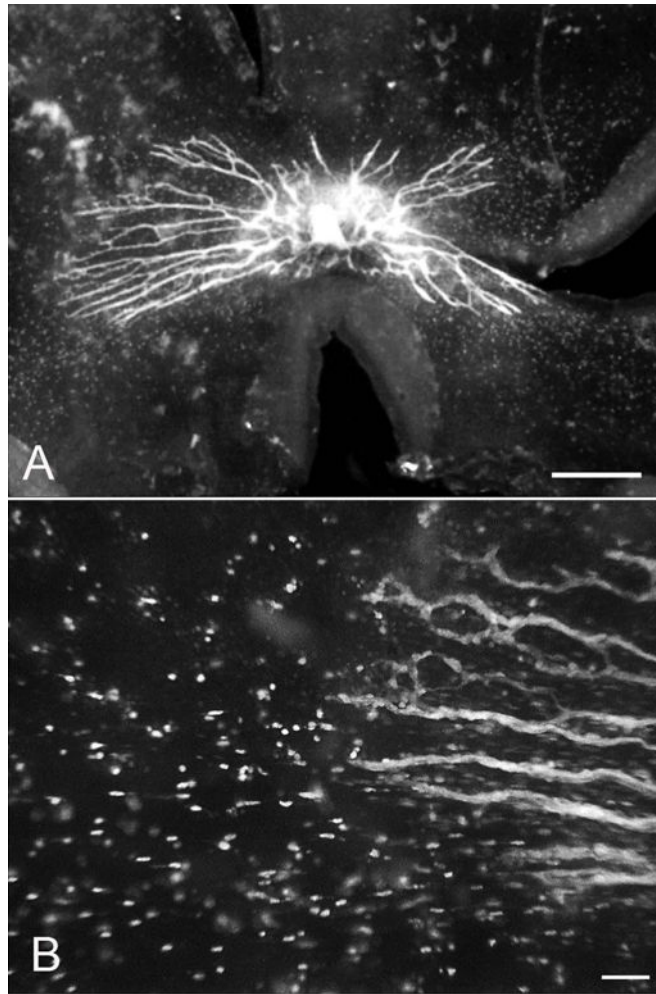


**Fig. 20.** Adenosine diphosphatase (ADPase) incubated 12 WG retina at low (A) and high (B) magnification. ADPase<sup>+</sup> angioblast precede the formed blood vessels by more than 1 mm in avascular retina. Individual angioblasts in focus in (B) are fusiform in shape. (A scale bar = 1 mm, B scale bar = 20  $\mu$ m).

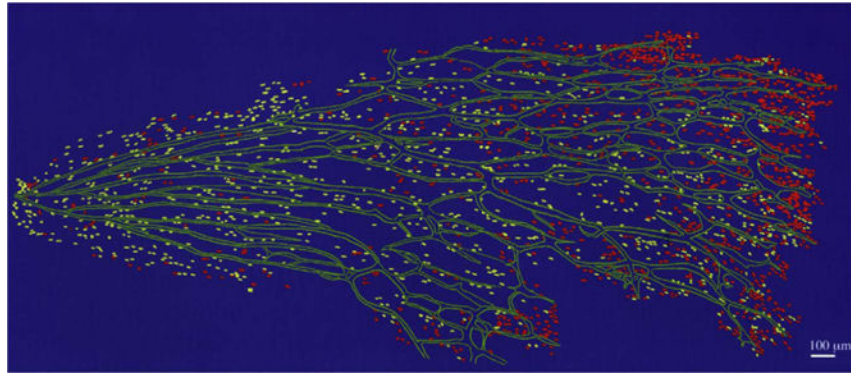


**Fig. 21.** A map of CD34<sup>+</sup> blood vessels (green), PAX2<sup>+</sup> astrocyte precursors (red), and PAX2<sup>+</sup>/GFAP<sup>+</sup> immature astrocytes (yellow) in a 14 WG retina (optic nerve to the left). The astrocyte precursors are just barely in advance of the blood vessels.

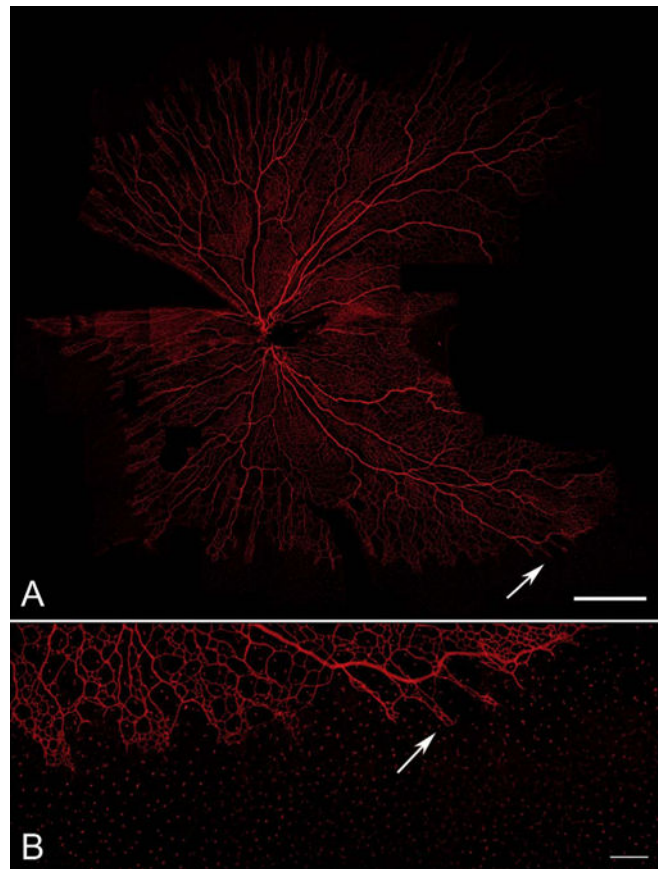


**Fig. 22.**

A 21 WG flat mount retina labeled with anti-CD39. At this age the vasculature forms a butterfly-like vascular system (A). Fields of the flat mount are missing on the right of the image in the area where the presumptive fovea will be. Even at this age at higher magnification (B), there are CD39<sup>+</sup> angioblasts in avascular peripheral retina that are coalescing to form the final superficial retinal vasculature. (A Scale bar = 2 mm, B Scale bar = 50 μm).

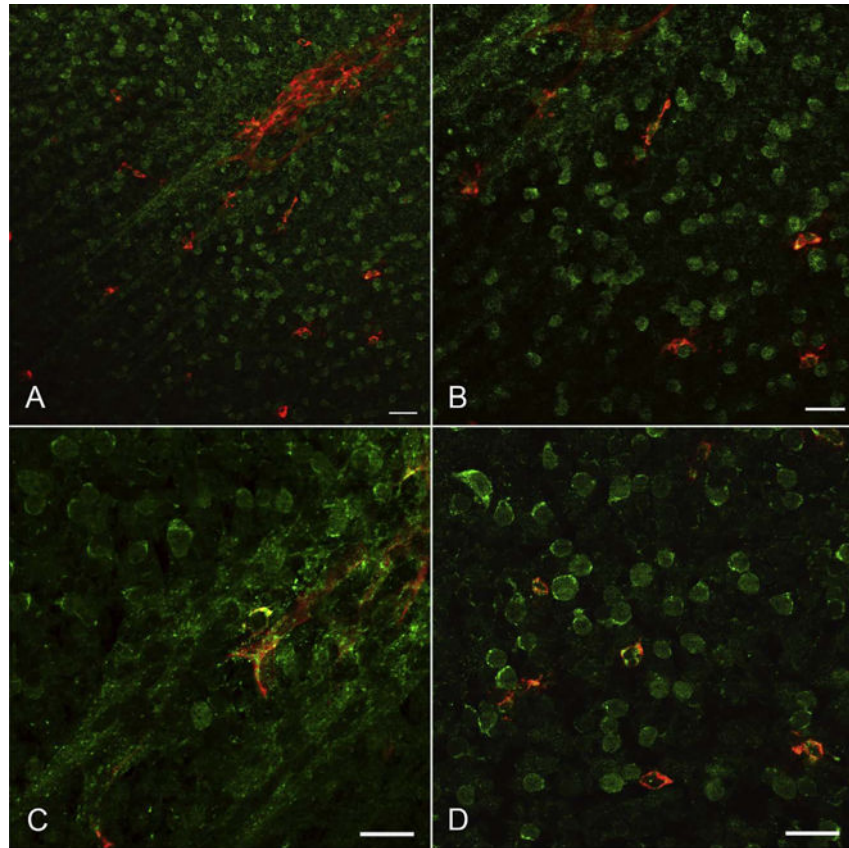


**Fig. 23.** Twenty-two WG flat mount retina labeled for CXCR4 (green) and CD39 (red). CD39<sup>+</sup> angioblasts are in advance of formed blood vessels (arrow) and appear to align with the formed cords. Many angioblasts are CD39<sup>+</sup>/CXCR4<sup>+</sup> (yellow). (A & B Scale bar = 20  $\mu$ m).

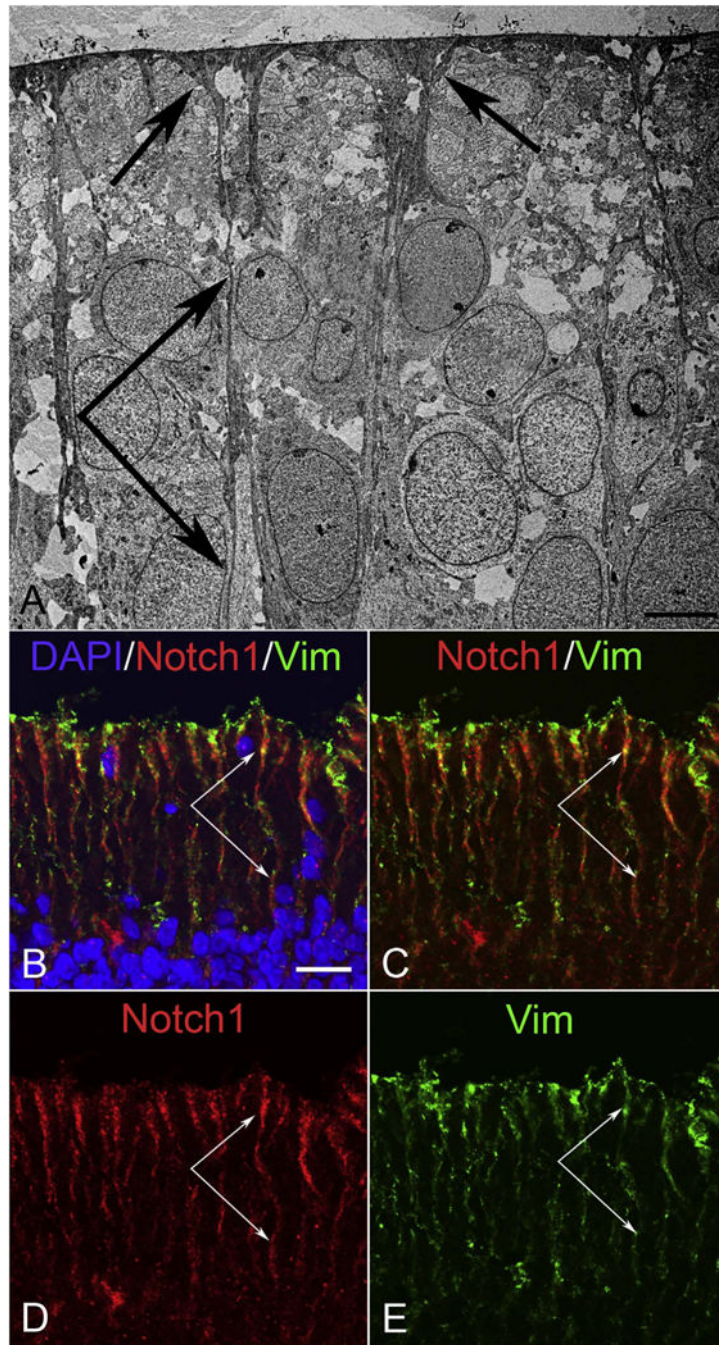


**Fig. 24.** Ultrastructure of inner retina at 9 WG (A) and immunohistochemistry of inner retina at 12 WG (B–E). (A) Inner Muller cell processes and foot pads are present at 9 WG in innermost retina. (B–E) Immunolabeling for Notch 1 (red) and vimentin (Vim, green) demonstrates that Notch1 is prominently expressed by vimentin<sup>+</sup> Muller cells at 12 WG in innermost retina. (Scale bar in A = 5  $\mu$ m, B–D = 20  $\mu$ m).

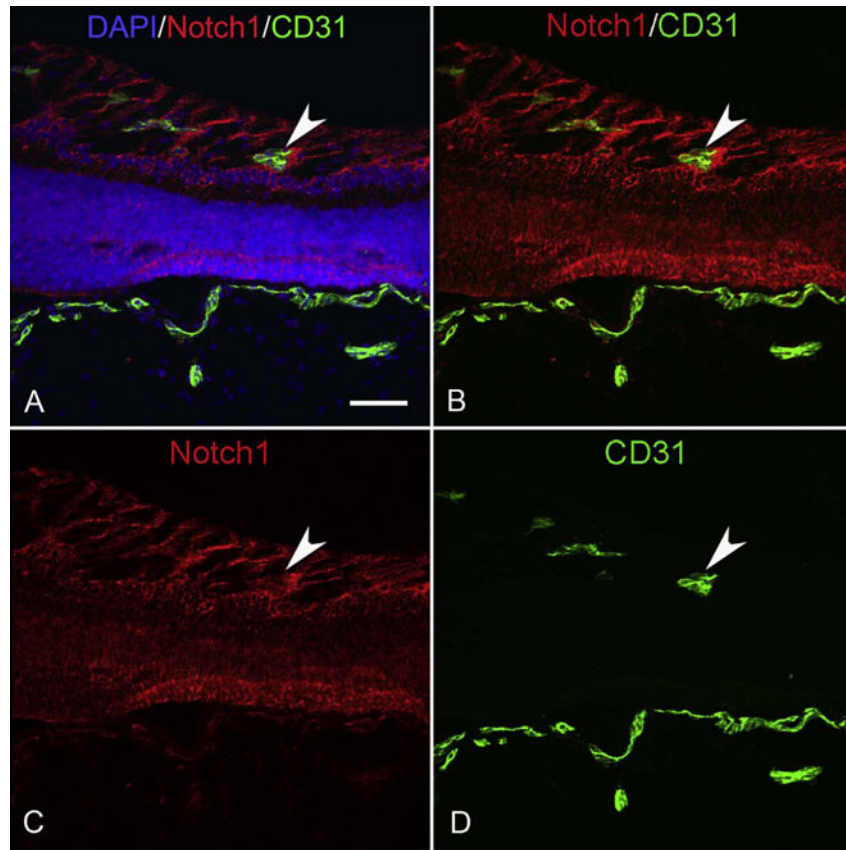


**Fig. 25.** Cryosections from a 17 WG eye that was labeled for Notch1 (red) and CD31 (green). Notch1 is prominently expressed by Muller cells, which appear to be forming spaces in which retinal blood vessels (CD31<sup>+</sup>) traverse (arrowhead). The choroidal vasculature is also CD31<sup>+</sup> (bottom). (Scale bar = 50  $\mu$ m).

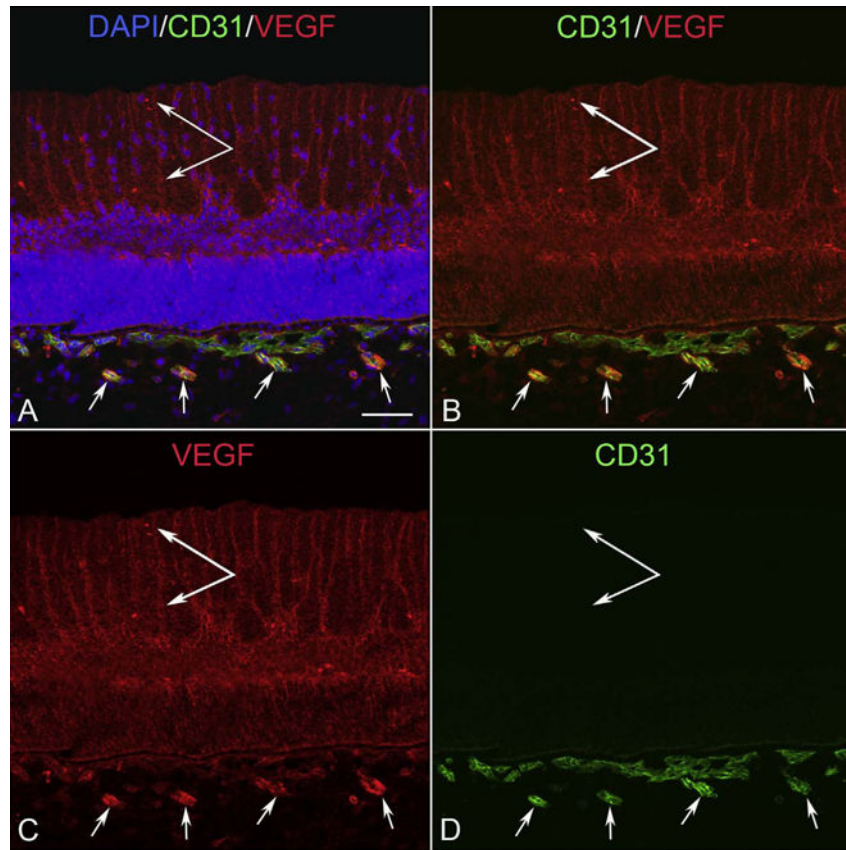


**Fig. 26.** VEGF localization at 12 WG. VEGF was prominently localized to apparent Muller inner processes (double arrow), the inner neuroblastic layer in retina, and in intermediate blood vessels in Sattler's layer of choroid that are developing at this time. There is less VEGF in primitive choriocapillaris. (Scale bar = 50  $\mu$ m).

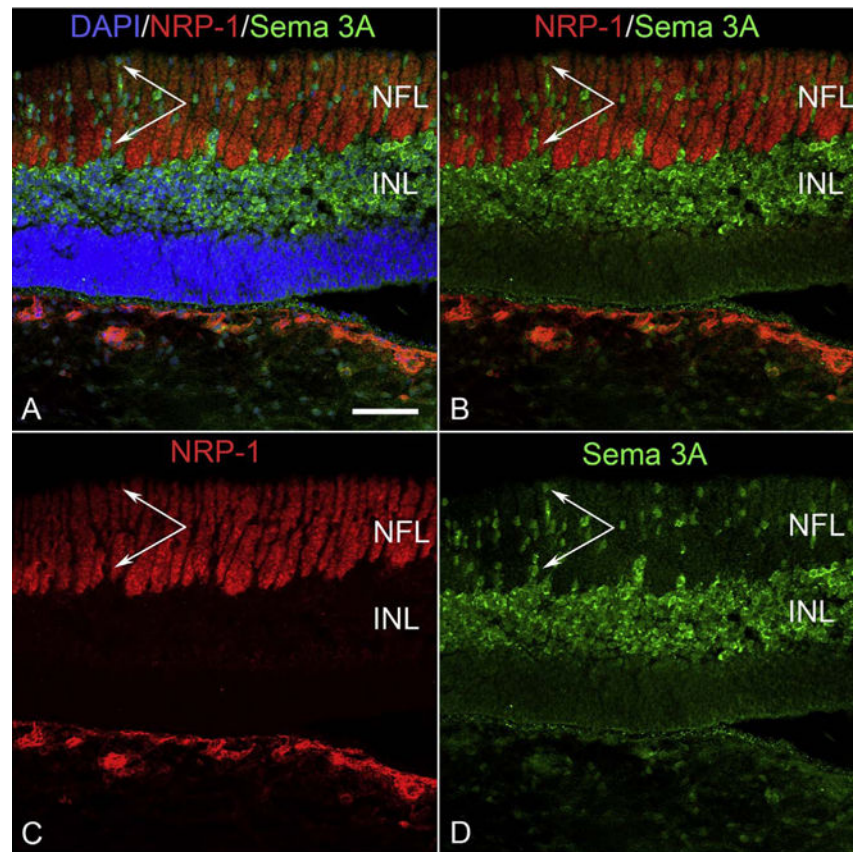


**Fig. 27.**

Cryosection of 12 WG eye labeled for neuropilin1 (NRP-1, red) and semaphorin 3A (Sema 3A, green). NRP-1 is prominently expressed by axons in inner retina and choroidal blood vessels (bottom). Sema 3A is predominantly expressed by cells in the inner neuroblastic layer but also by single angioblast-like cells in inner retina that associate with NRP1<sup>+</sup> axons (paired arrows). (Scale bar = 50  $\mu$ m).

**Table 1A**

Mechanism of vascular development in human versus mouse.

<b>Vasculature</b>	<b>Human</b>	<b>Mouse</b>
Fetal vasculature of vitreous	Hemovasculogenesis	Angiogenesis
Choriocapillaris	Hemovasculogenesis	Angiogenesis?
Superficial retina	Vasculogenesis	Angiogenesis
Deep retina	Angiogenesis	Angiogenesis

Author Manuscript

Author Manuscript

Author Manuscript

Author Manuscript

**Table 1B**

Guidance for superficial retinal vasculature in human versus mouse.

<b>Cell</b>	<b>Human</b>	<b>Mouse</b>
Astrocytes	N/A	Notch-1/VEGF <sub>164</sub>
Muller cells	Notch/VEGF <sub>164</sub>	?
Ganglion cell axons	NRP-1	Sema3a
Angioblasts (man) or tip endothelial cells (mouse)	Sema3a	NRP-1

(NRP-1 = neuropilin-1; Sema3a = semaphorin 3a; N/A = not applicable).

Author Manuscript

Author Manuscript

Author Manuscript

Author Manuscript